INVESTIGATING LIGAND INTERACTIONS AND DYNAMICS ON THE MEMBRANE PROTEOME THROUGH MEMBRANE MIMETIC THERMAL PROTEOME PROFILING (MM-TPP)

by

Rupinder Jandu

B.Sc., McMaster University, 2022

A THESIS SUBMITTED IN PARTIAL FULFILLMENT OF

THE REQUIREMENTS FOR THE DEGREE OF

MASTER OF SCIENCE

in

THE FACULTY OF GRADUATE AND POSTDOCTORAL STUDIES

(Biochemistry and Molecular Biology)

THE UNIVERSITY OF BRITISH COLUMBIA

(Vancouver)

April 2025

The following individuals certify that they have read, and recommend to the Faculty of Graduate and Postdoctoral Studies for acceptance, the thesis entitled:

INVESTIGATING LIGAND INTERACTIONS AND DYNAMICS ON THE MEMBRANE PROTEOME THROUGH MEMBRANE MIMETIC THERMAL PROTEOME PROFILING (MM-TPP)

submitted by Rupinder Jandu in partial fulfilment of the requirements for

the degree of Master of Science

in Biochemistry and Molecular Biology

Examining Committee:

Dr. Frank Duong van Hoa, Professor, Biochemistry and Molecular Biology, UBC

Supervisor

Dr. Seth Parker, Professor, Biochemistry and Molecular Biology, UBC

Supervisory Committee Member

Dr. Thibault Mayor, Professor, Biochemistry and Molecular Biology, UBC

Supervisory Committee Member

Dr. Robert Molday, Professor, Biochemistry and Molecular Biology, UBC

Additional Examiner

Abstract

Membrane proteins (MPs) are central to numerous cellular processes and represent key targets in drug discovery, yet their characterization can be challenging due to their hydrophobic nature and reliance on detergents for solubilization. Traditional workflows may destabilize MPs, hindering the study of their ligand interactions and downstream effects. In this thesis, we develop a novel membrane mimetic-based thermal proteome profiling (MM-TPP) workflow that aims to overcome these challenges by enabling the investigation of ligand-specific interactions on membrane proteomes in a detergent-free environment. Using peptidisc, we successfully capture integral membrane proteins (IMPs) into water-soluble libraries, facilitating downstream thermal proteome profiling. Using ATP and vanadate together (ATP-VO_4) as ligands, we validate the approach in both bacterial cells and mouse organ. Our results highlight ATP-VO_4-mediated stabilization of IMPs such as the bacterial ABC transporters MsbA and LolCD. As well as liver transporters like FATP2/SLC27A2 and BSEP/ABCB11. Beyond small-molecule ligands, MM-TPP highlights the effects of co-captured lipids on protein stability, underscoring the broader scope of this methodology. Additionally, MM-TPP has the potential to detect off-target stabilization effects of ATP derivatives, such as ADP, on non-ATP-binding proteins. showcasing its ability to uncover ligand metabolism and downstream interactions. This thesis establishes an introduction to MM-TPP as a basis for membrane proteome characterization.

Lay Summary

Membrane proteins (MPs) are vital for many cellular processes and are key targets for drug development. However, studying these proteins is challenging due to their low abundance and reliance on detergents, which can introduce structural instabilities. This thesis presents a novel method, termed membrane mimetic-based thermal proteome profiling (MM-TPP), to study MPs in a more native-like environment. Through capturing MPs into peptidisc peptides, we generate a collection of the membrane protoeme which is water-soluble, functional, and in a detergent-free environment. MM-TPP enables the investigation of how small molecules can affect MPs' stability. This method revealed that ATP stabilizes transporters involved in moving molecules across membranes while also uncovering unexpected effects on other proteins. Additionally, MM-TPP highlighted the role of naturally interacting lipids in regulating protein activity and stability. By enabling the study of MP thermal stability, this research has the potential to characterise whole proteomes against ligands of interests.

Preface

The pET28-$_{his6}$MsbA constructs were cloned by Dr. Zhiyu Zhao. All the experiments presented in this work were conducted by Rupinder Singh Jandu (me). The design of the experiments was done in collaboration with Dr. Franck Duong, Dr. Frank Antony, and me. All mass spectrometry sample injections were done by Dr. Hiroyuki Aoki. All other sample preparation, data analysis and its presentation through figures and tables was done by me.

The results presented in chapters 3.1, 3.2, 3.4, and 3.5 have been published in:

Jandu, R. S., Al-Seragi, M., Aoki, H., Babu, M., & Hoa, F. D. van. (2025). Membrane mimetic thermal proteome profiling (MM-TPP) towards mapping membrane protein-ligand dynamics. *eLife*, *14*. https://doi.org/10.7554/eLife.104549.1

The results presented in chapter 3.3 has been published in:

Jandu, R. S., Yu, H., Zhao, Z., Le, H. T., Kim, S., Huan, T., & Hoa, F. D. van. (2024). Capture of endogenous lipids in peptidiscs and effect on protein stability and activity. iScience, 27(4). https://doi.org/10.1016/j.isci.2024.109382

Within this body of work, generative AI (such as ChatGPT) was only used to write Python code to aid in data analysis and figure creation through a Matplotlib workflow.

Table of Contents

List of Tables

List of Figures

List of Abbreviations

ABC – ATP-binding cassette

AP-MS – Affinity purification mass spectrometry

AS-MS – Affinity selection mass spectrometry

BSEP – Bile salt export pump

CETSA – Cellular thermal shift assay

CMC – Critical micelle concentration

Cryo-EM – Cryogenic electron microscopy

DARTS – Drug affinity responsive target stability

DB-TPP – Detergent-based TPP

DDC – Detergent direct capture

DDM – n-Dodecyl-β-D-maltoside

DHW – Detergent high wash

DLW – Detergent low wash

DSF – Differential scanning fluorimetry

EGFR – Epidermal growth factor receptor

ER – Endoplasmic reticulum

FRET – Förster Resonance Energy Transfer

GPCRs – G-protein coupled receptors

HDX – Hydrogen deuterium exchange

HPLC – High performance liquid chromatography

IMP – Integral membrane protein

ITC – Isothermal titration calorimetry

ITDR – Isothermal dose-response

LC-MS/MS – Liquid chromatography and (tandem) mass spectrometry

LDLR – Low density lipoprotein receptor

LFQ – Label-free quantification

LiP – Limited proteolysis

MM-TPP – Membrane mimetic-based thermal proteome profiling

MPs – Membrane proteins

MSP – Membrane scaffold protein

MS – Mass spectrometry

NMR – Nuclear magnetic resonance

NP-40 – Nonidet P-40

OATPs – Organic anion transporter proteins

pLDDT – Predicted local distance difference test

SLC – Solute carrier

SMALP – Styrene-maleic acid co-polymer lipid particles

SPROX – Stability of proteins from rates of oxidation

SPR – Surface plasmon resonance

TfR – Transferrin receptor

TMDs – Transmembrane domains

TPP – Thermal proteome profiling

Acknowledgements

This journey has been enriched by the guidance, support, and inspiration of many remarkable individuals whom I owe my gratitude. Foremost, I would like to thank my research supervisor, *Dr. Franck Duong*, for believing in me, and giving me the freedom to grow, learn, and develop as a researcher, communicator, and educator throughout my graduate school career. Entering this field with little biochemistry experience, you have pushed me to heights I once thought were unreachable. Your encouragement to work hard and think beyond the confines of the bench has been a cornerstone of my career.

To my thesis supervisory committee members, *Dr. Thibault Mayor and Dr. Seth Parker*, thank you for your insightful feedback and attention to detail which both challenged and improved not just my work, but my intellectual growth as well.

I would also like to express my deepest thanks to *Dr. Frank Antony*, who has always been a source of motivation in the lab and a friend who has always been a listening ear. Your passion for science and hard work has greatly inspired this work.

To *Yilun Chen*, a mentor who became a dear friend, your efforts to teach me everything I know about membrane protein biochemistry have been invaluable, and I will always be deeply grateful. I could not have asked for a better lab mate, without whom this work would not have been possible.

To my *parents, grandparents, and brother*, your guidance and support are the foundation of this work, forever cemented in its creation. This meek offering pales in comparison to the boundless love and blessings you have bestowed upon me.

To *Sarah*, without you there is nothing. Thank you for your unwavering love and support, for finding your way to me no matter the distance in between. Your presence has been my greatest strength, and your love, the light that has guided me through it all.

To *Django*, whose endless faith in me has been the fuel to accomplish my goals. Your joy for life and companionship means more than you can ever comprehend.

The work in this thesis was partly funded through the Natural Sciences & Engineering Research Council of Canada (NSERC) – Canada Graduate Scholarship Masters.

This work is dedicated to my grandfather, *Sardar Sukhmander Singh Jandu*.

An individual who always valued research and strived to better the world through knowledge.

ਕੁੰਭੇ ਬਧਾ ਜਲੁ ਰਹੈ ਜਲ ਬਿਨੁ ਕੁੰਭੁ ਨ ਹੋਇ ॥

Water remains confined within the pitcher, but without water,

the pitcher could not have been formed.

ਗਿਆਨ ਕਾ ਬਧਾ ਮਨੁ ਰਹੈ ਗੁਰ ਬਿਨੁ ਗਿਆਨੁ ਨ ਹੋਇ ॥੫॥

Just so, the mind is restrained by spiritual wisdom,

but without the Guru, there is no spiritual wisdom.

- *Guru Nanak Dev Ji (Sri Guru Granth Sahib, page 469)*

Chapter 1: Introduction

A uniting feature of all living beings is that they are made up of cells, where intricate chemical processes unfold. As American astronomer Carl Sagan eloquently spoke, "*we are a way for the universe to know itself."* In this sense, biochemical and molecular biology research can be viewed as a form of philosophy, a means to understand how one came and remains to be. French philosopher René Descartes famously stated, "*I think, therefore I am*," yet it is not only thought but in seeing, feeling, and experiencing do we truly become alive. It is the rhodopsin in our retinal cells that allows us to visually experience our world. The olfactory receptors lining our nasal cavities allow us to smell, and as the 2021 Nobel Prize laureates highlighted, it's the TRPV1 and PIEZO channels that allow us to experience physical touch and sensations (Caterina et al., 1997; Harraz et al., 2022; Hill et al., 2022). What unites these sensory experiences is that they rely on membrane proteins (MPs), present within the lipid bilayer in which all living cells conduct their physiology, and how all human beings experience the world.

1.1 The membrane protein landscape

Fundamental to all life is the cellular membrane. Although it constitutes just 6–12% of the cell's volume, lipid membranes form a complex biochemical environment fine-tuned to support its resident MPs (Alberts et al., 2015). Of this total, 2–5% is represented by the plasma membrane, the lipid bilayer that separates the intracellular from the extracellular environment. Unlike prokaryote cells, whose sole lipid bilayer is the plasma membrane, eukaryotic cells are intricately subdivided into functionally distinct, membrane-enclosed compartments called organelles. While the lipid bilayer provides the structural foundation of biological membranes, it is the embedded MPs that endow each cellular membrane with its characteristic functional

attributes (Babcock & Li, 2014). It is the total collection of proteins found embedded in these cellular membranes that can be referred to as the membrane proteome. Constituting 20 – 30% of the human genome, the membrane proteome represents a diverse collection of proteins representing receptors, ion channels, transporters, enzymes, and important structural components (Fagerberg et al., 2010).

Broadly speaking, the membrane proteome consists of three classes of proteins, integral MPs (IMPs), peripherally associated MPs, and lipid-anchored MPs. Of the three, IMPs are defined by domains that span across the lipid bilayer, hence commonly referred to as transmembrane proteins. These membrane-spanning domains are characterized by their secondary protein structures which consist of either α-helices or β-strands, giving rise to α-helical transmembrane proteins or β-barrels respectively. Some MPs possess both structures as well (Cymer et al., 2014). In the eukaryotic system, most MPs are synthetized and inserted into the endoplasmic reticulum (ER) membrane, the site of protein assembly and modification prior to being sent off to their final destinations (Shao & Hegde, 2011).

Transmembrane proteins commonly found in the plasma membrane or its equivalents (e.g., the inner membrane of gram-negative bacteria and inner membrane of mitochondria in eukaryotic cells) are predominately characterized by the α-helical structural motif, typically consisting of 20–30 amino acid residues. The α-helical structure is stable as it optimizes intramolecular hydrogen bonding within the peptide backbone and orients hydrophobic residues toward the lipid bilayer core (Heyden et al., 2012). An alternative strategy for protein insertion into membranes is the β-barrel structure, formed by hydrogen-bonding between neighbouring β-sheets which run antiparallel. The conformation generates a hollow pore, with the luminal wall dominated by hydrophilic amino acid residues, and hydrophobic residues exposed to the lipid bilayer (X. C.

Zhang & Han, 2016). This arrangement allows for selective permeability making it ideal for insertion into the outer membranes of gram-negative bacteria, mitochondria, and chloroplasts in plants (Fairman et al., 2011). Through the mechanism of polypeptide insertion into the membrane, α-helical transmembrane proteins can present multiple topologies determined by the number of transmembrane segments? (TMSs) in the polypeptide chain. Proteins with a single TMS are called single-pass proteins, while those with multiple TMSs form multi-pass proteins.

1.1.1 Role of membrane proteins in cell, tissue, and organ physiology

Much of the work presented in this thesis is conducted on the mouse - one of the most important mammalian model systems for basic, translational, and biomedical research ("The Mouse Genome," 2002). Specifically, the work focuses on the liver organ, which is of high pharmacological interest due to its role in drug metabolism and its unique depth of vascularization. Most liver-specific functions are performed by parenchymal hepatocytes, which make up to 80% of the total cell population and volume of the organ (Blouin et al., 1977). Faced with the complex task of detoxifying blood while simultaneously secreting and internalizing vast amounts of proteins and lipids, hepatocytes possess a complex yet finely tuned collection of MPs that aid in these functions.

Like all epithelial cells, hepatocytes have polarity that segregates an apical (canalicular) and basolateral (sinusoidal) plasma membrane domains – each composed of distinct channels and receptors. The sinusoidal domain receives all incoming blood, playing a vital role in mediating exchange between the liver and circulating blood (Schulze et al., 2019). This requires the sinusoidal membrane to maintain key lipid and nutrient scavenging receptors, such as the low-density lipoprotein receptor (LDLR) and transferrin receptor (TfR), the key iron absorption

receptor. These receptors internalize their respective molecules through receptor-mediated endocytosis. Within the hepatocyte membrane proteome, there are around 200 transporters of which 80% belong to the solute carrier (SLC) family (Wiśniewski et al., 2016). The SLC family is a collection of MPs that facilitate the transport of many ions and organic molecules such as sugars, amino acids, and vitamins to name a few. They function through passive transport or secondary active transport (Colas et al., 2016). At the sinusoidal membrane, members of the organic anion transporting polypeptide family (OATPs), including OATP1B1 (SLCO1B1) and OATP1B3 (SLCO1B3), play essential roles in the uptake of endogenous and exogenous compounds. Examples of such compounds are bile acids and pharmaceutical signaling molecules such as statins, which increase the abundance of LDLR at the membrane surface (Ciută et al., 2023). Other typical proteins with a transporter or carrier function include the passive glucose transporter 2 (GLUT2/SLC2A2) and the fatty acid transport protein 2 (FATP2/SLC27A2), which mediate the uptake of glucose and fatty acids, respectively. One of the most abundant carrier proteins in the plasma membrane is the sodium/potassium ion ATPase, a transporter comprising alpha and beta subunits that maintain ionic balance within hepatocytes (Kalxdorf et al., 2021). At the canalicular (apical) membrane, the bile salt export pump (BSEP/ABCB11) plays a vital role in secreting bile acids into bile canaliculi, a process essential for lipid digestion and cholesterol homeostasis (H. Liu et al., 2023). Dysfunction of BSEP is associated with cholestatic liver disorders, highlighting its pharmacological significance (Kubitz et al., 2012). Other member of the ATP-binding cassette (ABC) transporters such as MDR1, ABCC3, ABCC4, and ABCC6 actively efflux organic molecules, including bile components and xenobiotics, to support detoxification and bile formation (Schulze et al., 2019). Meanwhile, cytochrome P450 enzymes, localized to the endoplasmic reticulum membrane, are key mediators of phase I drug

metabolism, catalyzing oxidative reactions that render hydrophobic compounds more water-soluble and ready for excretion (Massart et al., 2022).

In addition to their transport and metabolic roles, hepatocyte MPs also mediate critical signaling processes. For example, insulin receptors (IR) on the sinusoidal membrane regulate glucose and lipid metabolism (W.-H. Lee et al., 2023), while epidermal growth factor receptors (EGFR) are involved in liver regeneration and repair (Berasain & Avila, 2014). Evidently, the liver's ability to perform its diverse functions relies on the specialization of its membrane proteome. Distinct regions of the liver express specific MPs tailored to key processes, such as metabolism, detoxification, and nutrient transport, ensuring the efficient partitioning of its physiological roles.

1.1.2 Challenges in studying membrane proteins

Although studying MPs to understand cellular function and physiology is paramount, there are several analytical challenges to overcome. One key challenge is that MPs are naturally less abundant compared to soluble proteins, since the cellular membrane only makes up 6 – 12% of the total cell volume (Alberts et al., 2015). Furthermore, even within the MP classification, abundance can very significantly based on their subcellular localization. For example, in liver hepatocytes, the plasma membrane constitutes just 2% of the total cell membrane compared to the ~51% from the endoplasmic reticulum (ER) (Alberts et al., 2015), logically resulting in a more pronounced detection of ER localized MPs. Consequently, this results in an underrepresentation of the membrane proteome in bottom-up proteomics analysis (Beck et al., 2011; Helbig et al., 2010). To augment their detection, plasmid-based overexpression of MPs is commonly uses but may also result in the production of cytoplasmic aggregates (referred to as

inclusion bodies) of the target protein due to misfolding, hydrophobic interactions, or saturation of cellular machinery and chaperones (Wagner et al., 2006, 2007). This production and detection bottleneck is even more pronounced with the pharmaceutically relevant protein family of G-protein coupled receptors (GPCRs) due to their unique membrane topology of 7 TMS and numerous post translational modifications. Consequently, GPCR overexpression strategies often require unphysiological fusion to stabilize proteins or replacements of whole domains for successful heterologous expression (Addis et al., 2024; Sarkar et al., 2008).

Beside their lower abundance, due to their hydrophobic properties and poor solubility under aqueous conditions, MPs readily aggregate under conventional proteomic sample preparation methods. Detergents are useful for extracting MPs from the lipid bilayer and maintaining their solubility in aqueous solution, however, individual proteins may respond differently depending on the detergent type and concentration, requiring an optimization step for detergent use (Kotov et al., 2019; Lenoir et al., 2018). Any optimization increases the protocol complexity when investigating proteins at the proteome level, where targeted detergent use can exclude specific protein types or subcellular localizations (Arachea et al., 2012). Series of native mass spectrometry analyses conducted by the Carol Robinson lab have also shown the innate propensity of detergents to strip “annular” or protein-associated lipids from purified MPs (Barrera et al., 2013; Bolla et al., 2019; Laganowsky et al., 2014). These lipids can play important roles in MP function as shown with phosphoinositides and specific GPCRs as well as cardiolipin and the SecYEG translocon to name a few examples (Corey et al., 2018; Kuo et al., 2020; Yen et al., 2018). Commonly, non-ionic surfactants are used for whole proteome solubilization in thermal proteome profiling analysis as well. These detergents have a propensity to be structurally altered at their respective cloud-point temperatures, a temperature at which the

micellar solution spontaneously forms a two-phase separation. (Berlin et al., 2023). Above these temperatures, micelle-embedded proteins can become subject to crowding, aggregation, and introducing intermolecular concentrations that influence protein structure and proteome stability (Berlin et al., 2023) Apart from the potential for MP instability from detergent exposure, loss of membrane complexes under prolonged detergent exposure can inhibit accurate MP characterization, as interactome studies have shown, rarely do MPs act as isolated entities in the membrane, rather most functions occur in complex with both soluble and other transmembrane proteins (Carlson et al., 2019; Young et al., 2024; Zorman et al., 2015).

Additionally, to their disruptive nature, the presence of detergents in protein samples is poorly compatible with liquid chromatography and tandem mass spectrometry (LC-MS/MS) as residual detergent can deteriorate chromatographic separation and lower the performance of the MS instrumentation. Detergent presence can also impact protease digestion efficiency prior to MS-analysis as detergent concentration and ionic strength can compromise protease efficiency (Danko et al., 2022). Common proteases used for MS-digestion, such as trypsin or Lys-C, target positively charged residues like arginine and lysine for proteolytic cleavage. Whereas high hydrophobic regions in MPs lack charged residues for proteolytic cleavage, and reliable protein identification and quantification is dependant on generating multiple unique peptides that cover the protein sequence. Ionic detergents ionize during MS-analysis (through electron spray ionization) which can suppress the ionization of peptides, leading to reduced sensitivity. Detergents association with peptides may also shift mass/charge ratios further impacting accurate protein identification (Behnke & Urner, 2023; N. Zhang & Li, 2004). Although many detergent removal protocols have emerged, they are implicit with further protein loss (Brough et al., 2024). Ultimately, the hydrophobicity and low abundances of proteins can quickly complicate the

accurate characterization of MPs, especially through global large-scale functional and proteomics studies (Eichacker et al., 2004).

1.2 Approaches for investigating ligand-protein interactions

Assessing ligand-interactions has historically been in the context of health interventions and drug discovery. Traditionally, new drugs were discovered through phenotypic screens – assays that observe meaningful changes in biological system in response to ligand exposure (Swinney, 2013). This approach required no pre-knowledge on the potential targets or pathways involved in the phenotype, historical examples include the discovery of insulin and penicillin, the former which researchers observed its administration to diabetic dogs relieved their high blood-sugar phenotype (Ligon, 2004; Vecchio et al., 2018). As the understanding of physiological pathways and diseased states advanced, further emphasis was given to target-based approaches, where researchers studied and identified specific genes and proteins involved in diseased states. The following section will explore the biochemical and biophysical assays developed to assess ligand interactions, specifically on proteins, through hypothesis driven target-based approaches.

1.2.1 Biochemical approaches

Numerous approaches exist which look to measure small molecule binding on larger proteins. One of the gold-standards in this regard is isothermal titration calorimetry (ITC) which directly quantifies the changes in heat capacity during ligand binding directly to a purified protein at a single temperature condition. An attractive aspect of ITC is that it is label-free (therefore does not introduce artifacts) and can provide data on multiple thermodynamic parameters (Rajarathnam & Rösgen, 2013; Renaud et al., 2016; Vu et al., 2021). As a ligand

binds to a protein, the formation or breaking of non-covalent bonds can either release or absorb heat, undergoing exothermic or endothermic reactions, respectively. The loss or gain of heat in the reaction is referred to as the change in enthalpy (ΔH). The incremental ligand exposure (titration) to the purified protein results in the saturation of the protein's binding sites – resulting in earlier exposures generating larger changes in heat compared to later. Under the appropriate model, observing how the heat changes with each successive ligand exposure can determine the binding affinity (and thus the binding constant (K_d)) and stoichiometry of the reaction. Analyzing MPs under ITC can come with two major drawbacks – the requirement of relatively large amounts of protein, as well as maintaining MPs folded and functional outside the native membrane. As detergents are commonly employed to achieve the latter, their presence can influence the thermodynamics of the ligand binding process or mask binding sites, resulting in inaccurate measurements (Rajarathnam & Rösgen, 2013).

Another increasingly sensitive and label-free approach for measuring ligand-protein interactions is surface plasmon resonance (SPR). As an optical method, SPR detects changes in the refractive index at the interface between an aqueous layer and a sensor surface (usually a thin sheet of gold). A laser, set to a specific wavelength, generates an electron standing wave, or plasmon, on the metal surface, creating a resonance effect (Motsa & Stahelin, 2023). In SPR experiments, the bait protein is immobilized on a metal surface via functional groups, hydrophobic interactions, or affinity tags such as histidine (metal chelation) or biotin (streptavidin binding) (Motsa & Stahelin, 2023). When the analyte flows over the immobilized protein, binding increases mass at the sensor surface, shifting the resonance angle of reflected laser light. This shift, recorded in real time, detects binding events (Renaud et al., 2016). The association phase occurs as binding increases, while the dissociation phase follows when a wash

buffer removes unbound analyte. Together, these curves reveal binding kinetics and affinity. Similar challenges are shared between SPR and ITC when analyzing MPs, specifically maintaining the MP in a native, functional state and purifying enough protein. An added complexity is maintaining this while immobilizing the MP to the sensor surface (Patching, 2014).

Fluorescence-based techniques also have their place as sensitive alternatives for discerning ligand-protein interactions. Differential scanning fluorimetry (DSF) measures the temperature at which a purified protein unfolds under thermal stress (Gao et al., 2020). As the protein denatures, its hydrophobic core is exposed, allowing fluorescent probes/dyes, such as SPYRO Orange, to bind these newly accessible regions, resulting in fluorescence of the dye. By plotting the increase in fluorescence over a temperature range, a melting curve is generated, providing the melting temperature (T_m) of the target protein. As ligand binding often stabilizes or destabilizes the target protein through inducing conformational change, DSF-based screens measure ligand-interactions based on T_m shifts. Naturally, MPs, which are rich in hydrophobic residues and rely on amphipathic molecules such as lipids and detergents for solubility, present a challenge due to background fluorescence from dye interactions. To overcome this, intrinsic protein fluorescence can be used as an alternative to monitor protein thermal stability without external dyes. This approach takes advantage of the natural fluorescent properties of residues with aromatic side chains (tryptophan, tyrosine, and phenylalanine) (Ghisaidoobe & Chung, 2014). As the MP unfolds, increase in light emission can reflect changes in the protein conformation, providing clearer melting profiles without the background interference (Gooran & Kopra, 2024).

Similarly, Förster Resonance Energy Transfer (FRET) is another fluorescence-based technique that can monitor interactions between proteins and ligands. FRET relies on the non-radiative energy transfer between two fluorophores that emit different wavelengths of light. The protein is labeled with a donor fluorophore while the ligand of interest is labelled with an acceptor, when a binding event occurs the two fluorophores are in very close proximity to each other (< 10nm). When donor fluorophore is excited by a specific wavelength of light, the energy transfer to the acceptor fluorophore can be detected. The labelling of MPs with these fluorophores can pose a challenge, as many reactive residues are found on regions embedded in the lipid bilayer or completely absent. Interestingly, through optimizing detergent usage, solubilization can expose larger portions of the protein providing more efficient labelling of fluorophores. Although detergents may increase the background noise of fluorescence, advents such as single molecule FRET have been shown to provide sensitive analysis of MP-ligand interactions (Bartels et al., 2021).

1.2.2 Biophysical approaches

While the biochemical approaches such as ITC, SPR, and fluorescence-based methods provide important information on ligand kinetics, binding affinities, and thermodynamic properties of these interactions, they lack important information on where exactly the ligand binds its target, and what are the consequences of ligand binding at the atomic level. Biophysical structural techniques allow us to examine precisely the conformation of ligand-protein complexes. As structural work is not a focus of this thesis, I will briefly describe common approaches. X-ray crystallography is a classic approach that provides atomic-level structural information through analyzing X-ray diffraction patterns when directed at a crystallized protein

sample. The X-rays themselves interact with electrons of the atoms that make up the protein molecule generating an electron density map that elucidates 3D structures. Thus, any ligands bound to the protein in the crystalline structure will also be projected onto the electron density map, providing the exact location and interacting residues of the ligand-protein complex (Maveyraud & Mourey, 2020). While MPs make up a third of the human genome, very few structures of MPs have been fully resolved, reaching only 3% of crystal structures in the Protein Data Bank (Martin & Sawyer, 2019; Renaud et al., 2018). Although approximately 80% of MP structures have been solved through X-ray crystallography (Kermani, 2021), there are difficulties in generating the crystal state with MPs, generally due to the incompatibility of hydrophobic surfaces in the aqueous crystallization solutions. Relying on detergents to remain soluble outside the lipid bilayer, maintaining stable and structurally viable MPs in detergent micelles can also pose a challenge during crystallization, especially in the nonuniformity of detergent micelles or lipid complexes that accompany the MP (Kermani, 2021).

These hurdles have allowed alternative techniques, like Cryogenic Electron Microscopy (Cryo-EM), to gain popularity for establishing MP structures with ligand-bound structures. Awarded the 2017 Nobel Prize in Chemistry, Cryo-EM determines the structure of biological macromolecules through non-crystalline conditions, beneficial for MPs that are difficult to crystalize. Instead, samples are rapidly frozen in liquid ethane, which generates a thin, vitreous ice sheet that captures MPs in near-native states, which can be coupled with detergent removal steps such as GraFix, as detergent micelles influence the uniformity of ice thickness (Renaud et al., 2018). Through freezing ligand-bound states, Cryo-EM has the benefit of detecting different conformational states in one preparation, which through computational sorting, can provide a dynamic view of ligand-protein interactions, as was shown with the catalytic activity of the F-

type ATPase (Zhou et al., 2015) and the human parathyroid hormone receptor (PTH1R) binding its endogenous ligand (L.-H. Zhao et al., 2019).

Lastly, nuclear magnetic resonance (NMR) spectroscopy utilizes the magnetic properties of atomic nuclei (particularly hydrogen) to determine the spatial arrangement of atoms in macromolecules. This data can provide detailed information on bonding interactions, distances between residues, and molecular dynamics of ligand binding (Liang & Tamm, 2016). NMR, as with Cryo-EM, also bypasses the need to crystalize the MP-ligand complex, and through solid-state NMR, allows the determination of large MP structures still embedded in the lipid bilayer, maintaining a true native state (Liang & Tamm, 2016). This approach has elucidated ligand binding pockets of a diverse collection of proteins such as the bacterial ABC transporter MsbA interacting with inhibitors (Spadaccini et al., 2018) and the mammalian neuropeptide receptor's dynamic binding of neuropeptide-Y (Z. Yang et al., 2018). Together, these structural-based biophysical techniques provide a comprehensive view or MP-ligand interactions, capturing both the static and dynamic aspects of complex-structure determination. As each method has its advantages and challenges, technical advances continue to enhance their applicability towards MPs and drug discovery. The combination of these techniques can offer a comprehensive approach for understanding the molecular basis of ligand binding and protein dynamics.

1.2.3 The Cellular Thermal Shift Assay

The Cellular Thermal Shift Assay (CETSA), developed by Dr. Martinez Molina, adapted traditional thermal shift assays – usually limited to purified protein samples – to enable the analysis of whole cells, cell lysates, and tissue samples, hence allowing the study of ligand binding and target engagement in a native cellular environment (Molina et al., 2013). CETSA is

based on the long-standing knowledge that, when heated, proteins denature and generally become insoluble. Upon heat treatment, highspeed ultracentrifugation (e.g. 15 minutes at 180,000*g*) separates the insoluble fraction from the soluble fraction and the remaining soluble protein can be quantified via immunoassays such as Western blots, or ELISA (if working with cells or tissues, samples will require lysis prior to isolation of soluble fraction) (Molina & Nordlund, 2016). Plotting the amount of soluble protein against the tested temperatures generates a melting curve from which a melting temperature (T_m) can be derived. In parallel, the sample material can be incubated with a small-molecule compound which may alter the thermal stability profile of the target protein. Shifts in the T_m can be inferred that the compound is binding to the protein of interest (Mateus et al., 2020).

Unlike thermal unfolding methods previously discussed (like DSF), CETSA is advantageous by its ability to maintain cells in an intact state, preserving biological factors of drug targeting such as cell permeability of the compound, intracellular protein complex formation (Bantscheff et al., 2011), and the presence of cellular cofactors (Becher et al., 2013). CETSA was further advanced to measure compound potency through isothermal dose-response (ITDR) CESTA, a valuable step forward in drug discovery research. Performed at a single temperature condition, the concentration of the small-molecule is incrementally increased to assess concentration-specific alterations in protein melting curves (Molina et al., 2013), often yielding reliable IC_{50} values that correlate with data generated from other methods.

While CETSA is a valuable technique for detecting small molecule binding to a protein, it was initially seen as low throughput, relying on immunoblotting for detecting target denaturation. This limitation restricts CETSA primarily to validating expected, known targets such as the Ca^{2+}-ATPase (SERCA2) with thapsigargin or the mitochondria-localized translocator

protein (TPSO) with alpidem (Kawatkar et al., 2019). To address this, CETSA has recently been coupled to a mass spectrometry-based workflow significantly improving throughput and the depth of data obtained. It has been utilized to analyze the effects of cancer drugs on apoptosis events (Ramos et al., 2024) as well as brassinosteroid effects on live *Arabidopsis thaliana* cells (Lu et al., 2022). This advancement allows CETSA not only to validate target engagement but also to reveal possible off-target interactions.

1.3 Introduction to proteomics

Mass spectrometry (MS)-based proteomics is a broad field that enables the study of protein sequences, abundances, subcellular localization, and protein–protein interactions, and much more (Aebersold & Mann, 2016; Bolla et al., 2019). MS instruments identify proteins by measuring mass-to-charge ratios (m/z) and signal intensities of ionized proteins or fragments, with applications ranging from analyzing single proteins to profiling thousands across complex biological samples. The work in this thesis utilizes one of the most widely used and accessible MS-based techniques: bottom-up proteomics (or commonly referred to as “shotgun proteomics”), performed using data-dependent acquisition (DDA). In bottom-up proteomics, proteins are extracted from complex samples (like cells, tissues, or biological fluids) and digested into peptides, using proteases, which are then analyzed by MS. “Bottom-up” refers to inferring protein-level information from peptide data, with untargeted proteomics aiming to identify and estimate the relative abundance of proteins without prior targeting. In DDA mode, the process begins with a full primary MS1 scan where peptide precursor ion information is recorded according to their signal intensities. Following this, peptides with high-ranking intensities are selected for fragmentation one by one, commonly referred to as MS2 in tandem

mass spectrometry (MS/MS), enabling downstream sequence analysis. Through DDA experiments, peptide abundances can be quantified through either label-based or label-free approaches. Label-free quantification (LFQ) relies on the MS1 intensities to generate a relative quantification. Although regarded as the gold standard, DDA methods may generate missing values due to potential low sampling efficiency in complex samples and the stochastic nature of precursor peptide selection, which limits downstream MS/MS reproducibility (B. Zhang et al., 2016). However, innovations in data processing, such as comparing spectral libraries (precompiled databases of experimentally derived MS/MS protein spectra) to accurately predict peptide retention times. Along with this, imputation techniques have allowed LFQ to remain one of the most efficient approaches to quantifying proteome differences through MS (Beer et al., 2017; M. Liu & Dongre, 2021). Peptides are more reliable than intact proteins for such studies due to their consistent sizes and compatibility with reversed-phase high-performance liquid chromatography (HPLC), which improves the resolution of protein identification (Shuken, 2023).

1.3.1 Common proteomics-based methods for investigating ligand-protein interactions

Arguably the simplest method for elucidating ligand-protein interactions is affinity-purification mass spectrometry (AP-MS), a technique that directly identifies physical interactions between proteins and ligands. Many different ligand types can be used in AP-MS including oligonucleotides, chemicals, lipids, or proteins, with one of the most commonly utilized ligands being antibodies (Dunham et al., 2012). Ligands or bait proteins are commonly immobilized on a solid support such as affinity resin. A biological sample, whether a purified protein or a complex cell lysate, is then incubated with the resin allowing for stable interactions to form. Through

successive washes which remove unbound proteins, binding partners can be eluted and directly analyzed through MS or first separated through gel-based systems prior to MS (X. Liu et al., 2020).

Affinity-selection mass spectrometry (AS-MS) has emerged as an alternative, high-throughput method capable of screening thousands of small molecule compounds on isolated GPCRs (Qin et al., 2018; Yen et al., 2017), macromolecular complexes (Petersen et al., 2016), and isolated organelles (X.-X. Yang et al., 2015). Along with immobilizing bait targets on a solid phase, AS-MS can also be accomplished through in-solution methods, where isolated samples are incubated with a compound library, followed by filtration/ultracentrifugation or size exclusion chromatography to separate unbound compounds from ligand-protein complexes. The bound ligands can also be liberated through exposure to denaturants such as detergent or organic solvents, which promote complex dissociation. The liberated small molecules can then be identified through their chromatographic retention times and exact mass calculations (Prudent et al., 2020). Both AP- and AS-MS are amenable to MPs through the inclusion of mild detergents (Prudent et al., 2020), although AS-MS has been conducted in proteins retained in their lipid bilayer, such as overexpressed human 5-hydroxy-tryptamine 2C receptor (5-HT_{2C}R). The isolated membrane fraction was not solubilized with detergent to release MPs from the lipid bilayer but were instead allowed to remain in the crude membrane fraction during compound library incubation (Qin et al., 2018).

Another methodology to assess ligand-protein interactions through proteomics is Drug Affinity Responsive Target Stability (DARTS). DARTS is based on upon the principle that ligand binding induces conformational changes in protein structures. Compared to an apo state, ligand binding influences the available sites that could be cleaved by non-specific proteases such

as proteinase-K or thermolysin. This mode of ligand-binding analysis is generally referred to as limited proteolysis (LiP) and has been utilized to measure protein stability upon small molecule binding as well as the effect of osmolytes on a proteome-wide scale (Pepelnjak et al., 2024). As a non-specific protease is exposed to the protein-ligand complex, much of the protein will remain intact as only available sites will be cleaved. The left over proteins can then by denatured and digested with trypsin or Lys-C, resulting in a measurable difference in generated protease-specific peptides between the ligand-treated and control group (Ferraro et al., 2022). To include MPs in DARTS analysis, the use of crude cell lysates allowed for the retention of membrane associated proteins, while the inclusion of 0.3% DDM and wheat germ agglutinin agarose beads in the lysis buffer increased the presence of cell surface/plasma membrane proteins (Malinovska et al., 2023; Piazza et al., 2020).

The stability of proteins from rates of oxidation (SPROX) is a method that measures protein stability changes upon ligand binding through monitoring oxidation of methionine residues through hydrogen peroxide exposure (Strickland et al., 2013). In SPROX, isolated proteins or lysates are exposed to a ligand and increasing amounts of denaturant. Common denaturants are urea or guanidine hydrochloride. Ligand binding can influence the rate of unfolding from denaturants exposure, which in-turn, affects the amount of methionine residues that are exposed to the environment and available for oxidation upon peroxide exposure. Oxidation of methionine to methionine-sulfoxide adds ~16 Daltons to the molecular mass of the residue, allowing for measurable shifts in the m/z ratio of digested peptides (Guan et al., 2003; Hoare et al., 2024).

Another approach is Hydrogen/Deuterium exchange (HDX), which can provide detailed information about local conformational dynamics and elucidate specific binding sites. HDX-MS

works on the principle that the hydrogens of the amide backbone in proteins can spontaneously exchange with the bulk deuterium in the surrounding buffer. Thus, hydrogens that are exposed to the solvent exchange more quickly while those involved in binding and bond-formation, exchange slowly or not at all (J.-J. Lee et al., 2015). In HDX experiments, deuterium labeling can be performed using two primary approaches: continuous labeling and pulse labeling. Pulse labeling is primarily applied to study protein folding pathways. Most HDX-MS studies, however, rely on continuous labeling to examine protein folding and structural changes by tracking differences in deuterium exchange kinetics. Continuous labeling allows researchers to monitor deuterium incorporation over time, offering insight into the protein's structural dynamics under various conditions. Recently, nine different small molecules were profiled against the β1-andrenergic receptor, to investigate how ligand-binding influences structural changes in this protein (Toporowska et al., 2024).

1.3.2 Thermal proteome profiling for investigating ligand-protein interactions

As mentioned in section 1.2.2, CETSA is a powerful method for investigating protein-ligand interactions in native cellular conditions or in cell lysates. However, it can be considered low throughput as single proteins are probed individually. To overcome this bottleneck, thermal proteome profiling (TPP) combines the principles of CETSA with quantitative MS-based proteomics, enabling a high-throughput approach to study protein stability and interactions on a proteome-wide scale (Savitski et al., 2014). Through analyzing the entire soluble proteome, TPP allows simultaneous assessment of the melting profiles and thermal stability of all detected proteins, making it possible to identify both target and off-target proteins in response to small-molecule binding. Protein stabilization or destabilization in the presence of a ligand is revealed

by shifts in melting temperature or changes in protein abundance at specific temperature points, which the latter is predominately used in this thesis work to identify binding events.

Additionally, the sensitivity of MS-based proteomics enables TPP to detect a range of interaction types that affect protein thermal stability, such as protein-protein interactions, metabolite binding, nucleic acid binding, and post-translational modifications like phosphorylation (Le Sueur et al., 2022; Mateus et al., 2020). TPP can be adapted to address various research questions. For instance, a temperature gradient (3 - 5°C intervals) allows for detailed thermal profiling, which can generate a melting curve of thousands of proteins. Dose- or time-dependent TPP can refine conditions for ligand interactions: in dose-dependent TPP, a constant temperature is maintained while varying ligand concentrations define optimal binding conditions, and in time-dependent TPP, samples are exposed to a ligand for varying periods, again at isothermal conditions, to determine the minimal effective exposure time (Mateus et al., 2017). Studies suggest that 3–5 minutes are generally sufficient to identify binding events across sample types. Advanced TPP methods, like 2D-TPP, further enhance the sensitivity by detecting subtle changes in thermal stability by combining temperature gradients with dose or time perturbations, albeit at the cost of larger sample numbers (Becher et al., 2016).

To circumvent large sample numbers, multiplexing with isobaric tandem mass tags (TMT) significantly reduces sample complexity by combining conditions within a single MS run. This method supports the simultaneous analysis of up to 16 temperature or dose conditions, enhancing throughput and quantification accuracy (Johnson et al., 2023; Li et al., 2020; Thompson et al., 2003; Werner et al., 2012). Incorporation of TMT multiplexing comes with an additional cost to MS analysis, yet it can conserve sample run times, reduce sample injections that can introduce variability, and ultimately improve the consistency of peptide quantification

across experimental conditions. Despite these attractive features, isobaric tagging can suffer from shortcomings in precision and accuracy. Precision can be impacted due to incomplete labeling, which can be due to pH restrictions as well as the complexity of the sample type. The imprecision of measurements can be explained at least in part by correlation with reporter ion signal intensity: the precision of measurements decreases as the signal-to-noise ratio of the reporter ion measurement decreases. This can result in costly and lengthy troubleshooting before carrying out full-scale studies. Although statistical analysis can mitigate imprecision, poor accuracy tends to be a more stubborn issue. The commonly accepted source of inaccuracy is that contaminants are co-selected at the same time as a target-peptide which results in MS/MS spectra containing reporter ions obtained from mixed sources, commonly presented as the "ratio compression" effect, which LFQ-based methods are immune to (A. L. Christoforou & Lilley, 2012; Savitski et al., 2013). This is underscored by the requirement of specific LC-MS/MS equipment to conduct analysis of TMT-labeled samples, and the common observation of data loss from co-isolation interference of tagged peptides, which ultimately reduces the dynamic range of detectable reporter ions (A. Christoforou & Lilley, 2011; Ting et al., 2011).

1.3.3 Membrane protein analysis in thermal proteome profiling

Traditionally, CETSA- and TPP-based approaches have relied on the extraction of cells with detergent-free buffers, biasing ligand interactions to mostly soluble, cytosolic, proteins. As MPs are prominent drug targets, this flaw in the methodology was initially corrected through the incorporation of mild non-ionic detergents like Nonidet P-40 (NP-40) or n-Dodecyl-β-D-maltoside (DDM) during cell extraction to improve membrane proteome coverage (Huber et al., 2015; Kalxdorf et al., 2021; Reinhard et al., 2015). The incorporation of detergents can occur at

the step of lysis, which allows for the retention of MPs within the cell lysate. While this approach has been effective, there is a growing consensus that even mild detergents may impact IMP structure, activity, and thermal stability, thereby potentially attenuating accurate drug-target identification (Berlin et al., 2023; Z. Yang et al., 2014; Ye et al., 2023). Subsequently, researchers have also seen success in conducting TPP with crude lysates, which keep the lipid bilayer intact and only introduce detergents after ligand exposure and thermal treatment (Perrin et al., 2020). While mild detergents are commonly used, this can potentially introduce the risk of resolubilizing any unfolded and aggregated proteins. When conducting TPP on whole cells, detergents can once again be introduced after thermal treatment. A creative example of this is cell-surface TPP (CS-TPP), where post-thermal treatment, whole cells are oxidized and underwent biotinylating to biotinylate cell-surface proteins. This allows for capture of plasma membrane localizing proteins once cell lysis is conducted in the presence of detergent (Kalxdorf et al., 2021).

1.4 Membrane mimetics

Although they have enhanced the field of membrane biochemistry, detergent use can negatively impact MP stability and function. Over the past two decades, various membrane mimetics (MMs) have been established to minimize or bypass the negative effects of detergents on IMP stability. These developments have allowed researchers to stabilize IMPs in native-like environments that are detergent-free yet rendering them completely water soluble (Young, 2023). Common examples of MM systems include amphipols, nanodiscs, peptidiscs, saposin-lipoprotein particles (Salipro), and styrene-maleic acid co-polymer lipid particles (SMALPs) (Young, 2023).

The most widely used MM is nanodiscs, small, water-soluble patches of lipid bilayer containing a membrane protein of interest encircled by two copies of an ApoA1-derived membrane scaffold protein (MSP) (Bayburt et al., 2002). Generating nanodisc captured proteins can come with its own challenges of matching the diameter of the MSP to the target MP, along with establishing the correct stoichiometric ratios of exogenous lipids:MSP:target protein which prevents proteome wide capture. Instead, nanodisc are generally utilized to purify single proteins that have been conjugated with affinity tags. SMALPs have garnered significant attention as they are the only MMs that do not require prior detergent solubilization of the crude membrane to capture MPs, hence often referred to as "Native Nanodiscs". Instead, SMALPs can directly excise and capture IMPs directly from the lipid bilayer, holding the potential to systemically capture the membrane proteome in detergent-free conditions. Unfortunately, these polymers have consistently showcased markedly lower efficiencies in extracting MPs compared to detergents (Mueller et al., 2023). Yet, recent proteome-wide quantitative extraction methods highlight the increased ability of these polymers to rival detergent extracts and improve membrane proteome wide capture (Brown et al., 2024)

1.4.1 Peptidisc technology

The peptidisc is a 37 amino acid amphipathic peptide derived from reversing the sequence of the ApoA1-mimetic nanodisc scaffold peptide. Peptidisc offers several advantages over popular MMs such as nanodisc and SMALP. Primarily, peptidisc exhibit a "one size fits all" property and is universally applicable by self-assembling around a diverse range of α-helical and β-barrel MPs from both eukaryotic and bacterial sources. Like nanodisc, peptidisc reconstitution relies on a primary detergent solubilization step. Through reducing the detergent

concentration below the critical micelle concentration (CMC) with peptidisc-supplemented buffer, multiple peptidisc peptides spontaneously orient themselves around the hydrophobic domains of MPs. Unlike nanodisc, peptidisc reconstitution is a streamlined process as it does not require the addition of specific phospholipids but can co-capture any protein-associated lipids (Jandu et al., 2024). To increase the functionality of the peptidisc, different functional groups can be conjugated to the peptide for various applications. Through the addition of his-tags, biotin-tags, or a dual-conjugate his-biotin tag, reconstituted proteins can be immobilized to resin, allowing for the enrichment of IMPs (Young et al., 2020; Z. Zhao et al., 2023) or facilitate bioanalytical applications like biolayer interferometry (Saville et al., 2019). Furthermore, peptidisc can be conjugated with fluorophores such as fluorescein.

Many different reconstitution methods exist to capture MPs with peptidisc, in this work two methods are extensively used, on-beads (Carlson et al., 2018) and on-filter (Carlson et al., 2019). The on-beads reconstitution method requires the detergent solubilization of a membrane containing an over-expressed protein tagged with an affinity tag (e.g., his-tag). Following solubilization, an ultracentrifugation step removes the insoluble fraction, and the soluble fraction is incubated with the respective chromatography resin to immobilize the target MP. After washing away the unbound material, an excess of peptidisc peptide is supplemented in detergent-free buffer to bring the detergent concentration below the CMC and facilitate peptidisc reconstitution. After washing away the excess peptidisc, the target MP can be eluted in a detergent free elution buffer and is ready for downstream structural or functional analysis. The on-filter reconstitution method also requires the detergent solubilization of a crude membrane but does not require the overexpression or conjugation of a protein.

Through on-filter, MPs can be reconstituted immediately following detergent solubilization, reducing detergent exposure time which helps retain protein-lipid interactions as well as protein complexes. Through placing the solubilized membrane into a centrifugal filter, it can be quickly diluted with detergent-free buffer. Multiple rounds of dilution and concentration steps results in formation of a water-soluble membrane protein library (peptidisc library). This efficiently stabilizes a functional membrane proteome and has been successful in capturing bacterial MPs (Young et al., 2020, 2022, 2023) as well as from eukaryotic sources (Antony, Brough, Orangi, et al., 2024; Antony, Brough, Zhao, et al., 2024).

1.5 Membrane Mimetic-based Thermal Proteome Profiling

Through the application of peptidisc reconstitution, we refined the TPP methodology to target IMPs in detergent-free peptidisc libraries, thereby establishing MM-based TPP (MM-TPP). This refined method leverages the purified membrane fraction to enhance the detection and profiling of IMP-ligand binding events, while eliminating the destabilizing effects of detergent presence on protein structure and function. The on-filter reconstitution approach is broadly compatible, making MM-TPP applicable across a range of sample types, including bacterial cultures, mammalian cell lines, and organ tissues. In addition, the use of peptidisc libraries facilitates the co-capture of protein complexes and associated lipids, which supports a more holistic, native-like environment for assessing ligand binding and its downstream functional effects. This integration of protein-lipid complexes aims to enhance the detection sensitivity for interactions within the membrane proteome, providing an innovative platform for drug discovery. As this approach is conducted in a detergent-free aqueous environment, it allows for seamless sample preparation for LC-MS/MS, bypassing the need for detergent removal

protocols that can result in additional sample loss. The incorporation of MMs into proteome wide ligand binding assays has yet to be shown and this work pioneers a novel methodology for functional profiling of MPs.

1.6 Aims and Scope

The work presented in this thesis seeks to bridge a gap in membrane protein characterization by enabling the investigation of ligand binding on whole, functional membrane proteomes in a detergent-free environment. By leveraging membrane mimetics, this research aims to establish a framework for studying membrane protein-ligand interactions and their downstream effects. The specific aims of this work are as follows:

1. **Develop a TPP Workflow with Membrane Mimetics**: Establish a TPP workflow that incorporates membrane mimetics to investigate ligand-specific interactions across the membrane proteome.
2. **Evaluate Ligand Metabolism and Off-Target Effects**: Assess the feasibility of MM-TPP in elucidating downstream effects of ligand metabolism, with a focus on understanding off-target effects of small molecules.
3. **Expand MM-TPP Applications**: Explore non-small-molecule-based determinants of thermal stability in membrane proteins, such as the role of co-captured lipids, in modulating protein stability and function.

The scope of this thesis encompasses the application of this novel MM-TPP pipeline to both prokaryotic systems, using *Escherichia coli* as a model, and eukaryotic systems, including organ tissue from *Mus musculus*. Through utilizing ATP as a model ligand, this work lays the

foundation for a novel approach to membrane proteome characterization, with implications for drug discovery and the broader field of proteomics.

Chapter 2: Materials Methods

2.1 Reagents

The *Escherichia coli* strains BL21 (DE3) and the pET28-his$_6$MsbA plasmid are sourced from our laboratory collection. Peptidisc (NSPr and His-Biotin-NSPr, purity >90%) was obtained from Peptidisc Biotech. Detergent N-dodecyl-β-d-maltoside (DDM) was purchased from Anatrace. Nickel-chelating agarose was sourced from Qiagen. Tryptone, yeast extract, NaCl, imidazole, boric acid, Tris-base, acrylamide 40%, bis-acrylamide 2%, imidazole, ATP, and TEMED were acquired from Bioshop Canada. Isopropyl β-d-1-thiogalactopyranoside (IPTG) was purchased from Bio Basic. Kanamycin was obtained from GoldBio. Malachite green was acquired from Sigma.

2.2 Harvest of *Mus musculus* liver

The C57BL/6 mice were kept in specific pathogen-free conditions and received humane care in compliance with the Canadian Council of Animal Care guidelines, and the animal protocol was approved by the Animal Care Committee of the University of British Columbia. The mouse organs were obtained from female mice. The authors acknowledge that they did not consider the impact of mouse sex at the time of the study design. The mice received standard chow. At the age of 12 weeks, the mice were sacrificed, and the liver was excised and placed in vials with ice-cold sterile phosphate-buffered saline (PBS) until processing.

2.3 Preparation of crude membranes

For *Escherichia coli*, wildtype *E. coli* BL21 (DE3) or His-tagged MsbA (pET28-$_{his6}$MsbA) *E. coli* BL21 (DE3) was grown in 1 L of LB medium. After 3 hours, cells were harvested by low-speed centrifugation (6000g, 6 min) and resuspended in Buffer A (50 mM Tris-HCl pH 7.8, 100 mM NaCl, 10% Glycerol) supplemented with 1 mM phenylmethylsulfonyl fluoride (1 mM). Cells were lysed through a microfluidizer (Microfluidics; 3 passes at 15,000 psi at 4 °C). Unbroken cells and large aggregates were removed by low-speed centrifugation (6000g, 6 min). The crude membrane fraction was isolated by ultracentrifugation (100000g, 45 min, 4 °C, Beckman Coulter rotor Ti70). Membranes were resuspended in Buffer A at 5 mg/mL and stored at -80°C for later use.

For *Mus musculus*, the excised liver organ was washed several times in ice-cold PBS to remove the blood and then minced and homogenized in ice-cold hypotonic lysis buffer (10 mM Tris–HCl pH 7.4, 30 mM NaCl, and 1 mM EDTA, 1× cocktail protease inhibitor, and 1 mM PMSF) using a tight-fit metal douncer. All subsequent steps were performed at 4 °C or on ice. After adding 10 mM $MgCl_2$ and 50 μg/mL DNase, the suspension was further dounced and incubated for 10 min. The swollen tissue suspension was lysed using a French press (3 passes at 500 PSI). Unbroken cells and nucleus fraction were removed by low-speed centrifugation (1200g for 10 min). The supernatant was collected and centrifuged at a higher speed (5000g, 10 min) to remove the mitochondrial fraction. The crude membrane fraction was then collected by ultracentrifugation (110000g, 45 min) in a Beckman TLA110 rotor. This membrane pellet was resuspended in 100 μL of 50 mM Tris, pH 7.9, 100 mM NaCl, and 10% glycerol (TSG Buffer) and stored at −80 °C until use.

2.4 Preparation of peptidisc library

For peptidisc library preparation, ~2 mg of crude membranes (either *E. coli* or *M. musculus*) was solubilized in 50 mM Tris, pH 7.9, 25 mM NaCl, and 1% DDM (Solubilization Buffer) for 30 min at 4 °C with gentle shaking. The insoluble material was pelleted by ultracentrifugation (180000g, 15 min). The detergent extract (500 µL) was then reconstituted by mixing it with a 3-fold excess (w/w) peptidisc peptide for 15 min at 4 °C. The sample was rapidly diluted to 15 mL in 50 mM Tris, pH 7.9 and 25 mM NaCl (Buffer A) over a 100 kDa cutoff centrifugal filter. The sample was concentrated (3000g, 10 min) to ~200 µL. This process was repeated for a total of three rounds of dilution and concentration to deplete DDM to an approximate concentration of 0.008% to complete peptidisc reconstitution. The peptidisc library was immediately used for downstream thermal proteome profiling.

2.5 Expression and purification of His-MsbA for thermal stability assay

Histidine-tagged MsbA (His-MsbA) was expressed, purified, and reconstituted in Peptidisc through the on-bead method as described in Angiulli et al. (2020) with slight modifications (Angiulli et al., 2020). Briefly, His-tagged MsbA (pET28-$_{his6}$MsbA) was produced in E. coli BL21(DE3) at 37°C in 1L of LB medium supplemented with 50 µg/mL kanamycin. The inducer IPTG (0.5 mM) was added during the exponential growth phase (OD_{600nm} ~ 0.4). After 3 hours, cells were harvested by low-speed centrifugation (6000g, 6 min) and resuspended in Buffer A (50 mM Tris-HCl pH 7.8, 100 mM NaCl, 10% Glycerol) supplemented with phenylmethylsulfonyl fluoride (1 mM). Cells were lysed through a microfluidizer (Microfluidics; 3 passes at 15,000 psi at 4°C). Unbroken cells and large aggregates were removed by low-speed centrifugation (6000g, 6 min). The crude membrane fraction containing MsbA was isolated by

ultracentrifugation (100000g, 45 min, 4°C, Beckman Coulter rotor Ti70). About 2 mg of MsbA-enriched membranes were solubilized with 1% DDM (w/v) for 30 min at 4°C. The detergent solubilized material was ultracentrifuged (180000g, 15 min, 4°C, Beckman Coulter rotor TLA55) to pellet insoluble material. The supernatant was incubated with Ni-NTA (150 µL) resin for 45 min at 4°C on a tabletop rocker. The resin was sedimented through centrifugation (2000g, 1 min) and washed three times with 1.5mL of Buffer A supplemented with 0.02% DDM and 30mM imidazole. After removing the excess buffer, the beads were resuspended in Buffer A containing Peptidisc peptide (1 mg/mL). The excess peptide was washed away with Buffer A. The protein was eluted with 600 mM imidazole in Buffer A and the concentration was determined through a Bradford reagent.

2.6 Preparation of different reconstitutions of His-MsbA in peptidiscs

In the Detergent Direct Capture (DDC) method, about 3 mg of MsbA-enriched membranes were solubilized with 1% DDM (w/v) for 30 min at 4°C. The detergent extract was clarified by ultracentrifugation (180000g, 15 min, 4°C) and an aliquot (1 mL) of the detergent extract (2 mg/mL) was mixed with a molar excess of peptidisc peptides (1 mg). The mixture was then rapidly diluted into 15 mL of Buffer A (50 mM Tris-HCl pH 7.8, 100mM NaCl, 10% Glycerol) before concentration over a nitrocellulose filter to a final volume of 500 mL (Millipore; 100 kDa cut-off, 3000g, 20 min, 4°C). The dilution and concentration process were repeated three times to decrease the detergent concentration to a calculated estimate of ~0.008% final. The mixture was then incubated on a tabletop rocker with the Ni-NTA resin (150 µL) for 1 hour at 4°C. The resin was sedimented (3000g for 3 min) and washed once with 10x-column volume (CV; 1.5 mL of Buffer A). The peptidisc-reconstituted MsbA (DDC-MsbA) was eluted in 200 µL of Buffer A + 600 mM Imidazole. The protein samples were directly used for downstream thermal stability and

ATPase assays or stored at -20°C before lipid analysis. In the Low-Wash and High-Wash methods, an aliquot (1 mL) of the detergent extract prepared above (2 mg/mL) was incubated with Ni-NTA resin (150 µL) for 1 hour at 4°C on a tabletop rocker. The resin was then sedimented and washed three times (DLW-MsbA) or ten times (DHW-MsbA) with 1.5 mL Buffer A supplemented with 0.02% DDM (i.e. 30 CV and 100 CV washes, respectively). The resin was then resuspended in 1 mL of Buffer A supplemented with the peptidisc peptides (1 mg). The resin was washed with 1.5 mL Buffer A to remove excess peptide. The peptidisc-reconstituted MsbA was eluted in Buffer A + 600 mM Imidazole (200 mL). Protein samples were directly used or placed at -20°C for short term storage. In the detergent purified method, the Low-Wash protocol was followed minus the peptidisc reconstitution step. The Ni-NTA bound MsbA is then eluted in Buffer A + 600 mM Imidazole + 0.02% DDM (w/v) to generate DDM-MsbA.

2.6.1 Thermal stability of altered lipidic states of purified His-MsbA

The peptidisc reconstituted protein sample concentration was adjusted to 0.5 mg/mL in 50mM Tris-HCl pH 7.8, 100mM NaCl. For DDM-MsbA, the same buffer contained 0.02% DDM. Aliquots (50 µL) were placed in 200 µL thin-wall PCR tubes (Diamed) and placed in a thermocycler with the block and lid temperatures set to 50°C. Samples were removed from the heat block every two minutes over a time course of 10 minutes. Samples were transferred to a 1.5 mL polypropylene tube before ultracentrifugation (180000g, 15 min, 4°C, Beckman Coulter rotor TL-55). The soluble fraction (15 µL) obtained for each time point was analyzed by SDS-PAGE and stained with Coomassie Blue. Densitometry of the protein band intensity was performed using the software Image J.

2.7 MM-TPP on membrane proteomes

Peptidisc membrane protein library was split into two equal aliquots (50 – 100 µL) representing the control and treatment samples. Both the treatment and control groups were supplemented with 5 mM $MgCl_2$ and 0.2 mM VO_4. Treatment samples were then exposed to a final concentration of 2 mM ATP while the control received an equal volume of ddH_2O. For experiments with AMP-PNP, 2 mM AMP-PNP was substituted in place of ATP. The samples were incubated for 10 minutes at room temperature, divided into four aliquots and transferred into 0.2 mL PCR tubes. Each sample was heated in parallel for 3 minutes to their respective temperature (51-64°C). Subsequently, the samples were centrifuged at 180000g for 15 minutes at 4°C and the supernatant was collected for in-solution digestion.

2.8 ATPase assay on purified MsbA

The ATPase activities were determined using the Malachite green assay (Lanzetta et al., 1979) with few modifications. For peptidisc reconstituted MsbA, 5 mg was incubated at 37°C in 200 ml of reaction buffer (50 mM Tris-HCl pH 7.8, 100 mM NaCl, 5 mM MgCl2) containing 2 mM of ATP, plus 0.02% DDM in the case of the DDM-MsbA assay. Aliquots (20 µL) were taken every two minutes and mixed with 500 mL of Malachite green solution containing 0.05% Triton X-100. Light absorption at 660 nm was measured after 10 min incubation at room temperature. The ATPase activity was calculated using a standard curve generated with a phosphorous standard solution. The ATPase measurements were performed in triplicate to establish the standard deviation (SD). Initial rates were calculated using the linear part of the curve and dividing the molar amount of free phosphate produced by the molar amount of MsbA over a period of 10 min.

2.9 Mass spectrometry sample preparation & LC-MS/MS analysis

Equal volumes of supernatants from the treatment and control groups were treated with 6 M urea at room temperature for 30 min before reduction with 10 mM fresh dithiothreitol (DTT) for 1 h. Alkylation was performed with 20 mM iodoacetamide (IAA) in the dark at room temperature for 30 min, followed by a second round of reduction via 10 mM DTT for 30 min. The urea was diluted to 1 M with Buffer A. Trypsin digestion was performed with an enzyme/protein ratio of 1:100 at room temperature for 24 h. The tryptic peptides were acidified to pH 3 with 10% formic acid and desalted using hand-packed stage tips of C18 resin. The peptides were eluted with 80% acetonitrile and 0.1% formic acid and were dried by vacuum centrifugation. The analysis of tryptic peptides was performed in a NanoLC connected to an Orbitrap Exploris mass spectrometer (Thermo Fisher Scientific) was used for the analysis of all samples. The peptide separation was carried out using a Proxeon EASY nLC 1200 System (Thermo Fisher Scientific) fitted with a custom-made C18 column (15 cm x 150 μm ID) packed with HxSil C18 3 μm Resin 100 Å (Hamilton). A gradient of water/acetonitrile/0.1% formic acid was employed for chromatography. The samples were injected into the column and run for 180 minutes at a flow rate of 0.60 μL/min. The peptide separation began with 1% acetonitrile, increasing to 3% in the first 4 minutes, followed by a linear gradient from 3% to 23% acetonitrile over 86 minutes, then another increase from 24% to 80% acetonitrile over 35 minutes, and finally a 35-minute wash at 80% acetonitrile, and then decreasing to 1% acetonitrile for 10 min and kept 1% acetonitrile for another 10 min. The eluted peptides were ionized using positive nanoelectrospray ionization (NSI) and directly introduced into the mass spectrometer with an ion source temperature set at 250°C and an ion spray voltage of 2.1 kV. Full-scan MS spectra (m/z 350–2000) were captured

in Orbitrap Exploris at a resolution of 120,000 (m/z 400). The automatic gain control was set to 1e6 for full FTMS scans and 5e4 for MS/MS scans. Ions with intensities above 1500 counts underwent fragmentation via nanoelectrospray ionization (NSI) in the linear ion trap. The top 15 most intense ions with charge states of ≥ 2 were sequentially isolated and fragmented using normalized collision energy of 30%, activation Q of 0.250, and an activation time of 10 ms. Ions selected for MS/MS were excluded from further selection for 3 seconds. The Orbitrap Exploris mass spectrometer was operated using Thermo XCalibur software.

2.10 Data & statistical analysis in MaxQuant & Perseus

Raw mass spectrometric files were analyzed in the MaxQuant environment, version 2.4.1.0. The MS/MS spectra were searched using the Andromeda search engine against the UniProt-mouse protein database (UP000000589, December 2021, 55086 entries) and UniProt-escherichia coli protein database (UP000002032, July 2009, 4156 entries). Precursor mass and fragment mass were set with initial mass tolerances of 20 ppm for both the precursor and fragment ions. The search included variable modifications of asparagine/glutamine deamidation, methionine oxidation, and N-terminal acetylation and a fixed modification of carbamidomethyl cysteine. The maximum number of missed cleavages was set at two, and the maximum modifications/peptide and minimum peptide length were set at six amino acids. The UniProt database was also concatenated with an automatically generated reverse database to estimate the false discovery rate (FDR) by using a target decoy search. The false discovery rate (FDR) was set at 0.01 for the peptide spectrum match (PSM) and protein identifications. When identified peptides were all shared between two proteins, they were combined and reported as one protein group. For relative quantification, MaxQuant's label-free quantification method, LFQ, was enabled.

Each treatment and control sample were collected from three technical replicates. The ProteinGroups.txt output file from MaxQuant was exported into Perseus v1.6.15.0 for downstream analysis. In-house functions of Perseus were used to identify and remove protein groups from the reverse decoy database, those marked as potential contaminants, or those only identified by a post-translational modification site. The remaining intensity, and label-free quantification (LFQ) intensity were $\log_2$ transformed and normalized to the mean Peptidisc peptide intensity value. To identify proteins with significant change in thermal stability, a Student's t-test was conducted with a within-groups variance, s0, set to 0.1. The test was applied to data filtered for proteins that had at least three valid LFQ intensities in either the treatment or control group. The remaining undefine intensity values were imputed from a normal distribution with a downshift of 1.8 standard deviations from the total sample mean and a width of 0.3 times the sample standard deviation. To determine significantly stabilized or destabilized as a result of ligand exposure, proteins with a p-value < 0.05 and abundance fold change > 1.8 or < -1.8 were considered as the direct or indirect candidates of ligand-binders. Only proteins with at least two unique peptides were considered for this calculation. To visualise the temperature-dependent peptide intensity data, the smoothed curves were generated using the Piecewise Cubic Hermite Interpolating Polynomial (PCHIP) method. PCHIP interpolation was applied to the mean intensity values of each experimental group across the temperature gradient. Figures were generated through NumPy, Matplotlib, and Pandas Python coding language.

2.11 Protein annotation

The protein list obtained from MaxQuant was subjected to a Gene Ontology (GO) term analysis using the UniProtKB database to identify proteins with the GO-term "membrane". Proteins from

this group were extracted in FastA format and the Phobius web server ((http://phobius.sbc.su.se/) was utilized to predict the number of transmembrane segments (TMS). Any protein with at least one TMS was classified as an IMP. Protein with no TMS but with the GO annotation "membrane" was classified as a peripherally bound protein, all other proteins were considered as soluble proteins. To assess molecular functions of significantly stabilized IMPs, the Gene Ontology Molecular Function ('GO_MF_Direct/GO_MF_FAT') was used through DAVID Bioinformatics (https://david.ncifcrf.gov/). An EASE score of 0.05 was applied to test for significant GO terms based on a p-value cut-off of 0.05 after Benjamini-Hochberg correction.

2.12 Data availability statement

The MS-based proteomics data of this study have been deposited to the ProteomeXchange Consortium via the PRIDE partner repository and are available through the identifier PXD055093.

Chapter 3: Results

3.1 Validation of MM-TPP in *Escherichia coli*

The workflow for membrane mimetic-based thermal proteome profiling (MM-TPP) is illustrated in Figure 1. Initially, the isolated membrane fraction is solubilized in a non-ionic detergent to extract the membrane proteome. The detergent-solubilized mixture is then subjected to centrifugal filtration, which removes detergent micelles while facilitating the Peptidisc reconstitution of membrane proteins (MPs). This process results in a water-soluble "library" and has been utilized in previous studies (Antony, Brough, Zhao, et al., 2024; Carlson et al., 2019; Z. Zhao et al., 2023). The peptidisc library is divided into two equal volumes: one exposed to the ligand of interest (treatment) and the other to a vehicle (control). Each sample is then split and subjected to a series of controlled temperature treatments for 3 minutes to induce thermal denaturation and protein precipitation. The soluble fraction is then isolated through ultracentrifugation before analysis by tandem mass spectrometry (LC-MS/MS). Proteins identified with at least two quantitative unique peptides are retained for proteomic analysis. Significant changes in protein abundance between the ligand-treated and control groups are determined using a p-value threshold of < 0.05 and an abundance fold-change threshold of > 2 or < -2, as described. Proteins meeting these criteria are identified as direct or indirect targets of the ligand.

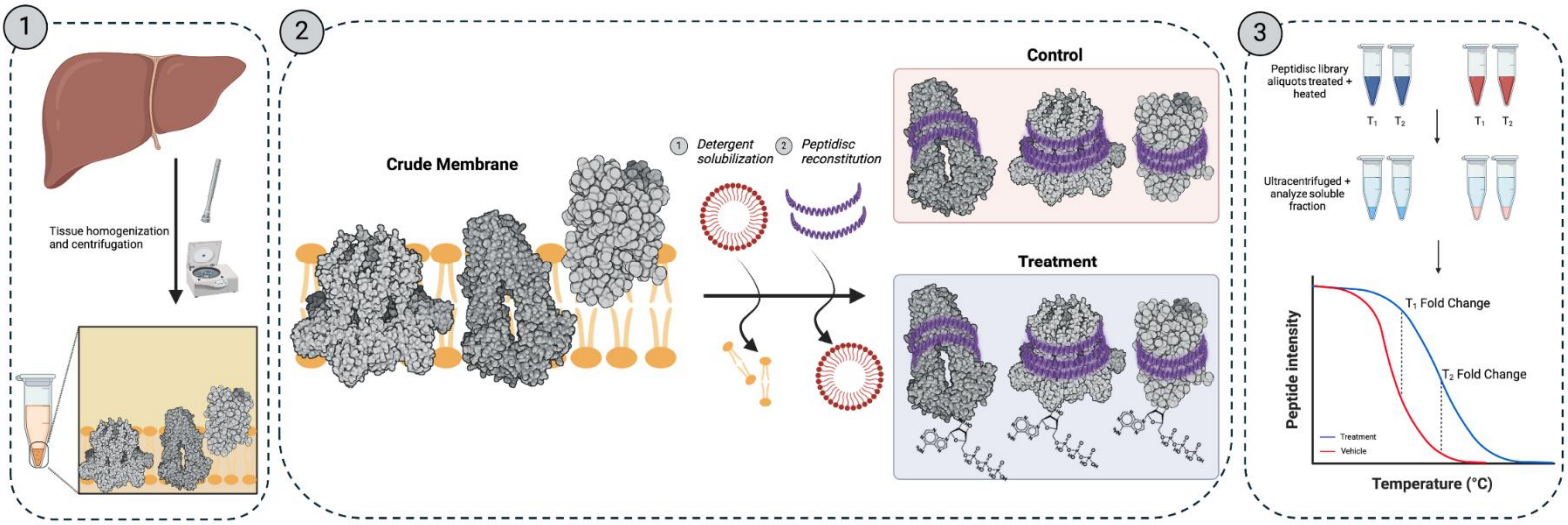

Figure 1: The Membrane Mimetic-Thermal Proteome Profiling (MM-TPP) experimental workflow. 1) Crude membranes are prepared from the liver organ. **2)** Integral membrane proteins (IMPs) are solubilized with detergent and reconstituted in the Peptidisc library. The water-soluble library is exposed to the ligand of interest (treatment) or corresponding vehicle (control)**. 3)** Protein samples are heated at specific temperatures to induce precipitation, followed by ultracentrifugation. The soluble fraction is analyzed by mass spectrometry to detect changes in protein abundances between treatment and control sample

As a validation step, we determined the thermal stability of the purified bacterial ABC transporter MsbA in the presence of ATP and vanadate (VO_4). Vanadate is a potent inhibitor of the ABC transporter family that mimics the transition state of phosphate during ATP hydrolysis, effectively locking the transporter in a specific conformation (Lyu et al., 2022). Accordingly, the SDS-PAGE analysis reported an increased thermal stability of MsbA in the presence of these ligands (Figure 2A). Further examinations involved an assessment of the ATP-VO_4 effect on the membrane protein library derived from wild-type *E. coli*, where MsbA is present at endogenous levels (Figure 2B). Results revealed that ATP-VO_4 significantly stabilizes MsbA at temperatures

of 51°C and higher (Figure 2C). Notably, at the maximum temperature tested, 61°C, the volcano plot indicated that MsbA's stabilization occurs alongside two other IMPs, FtsK and LolC (Figure 2D). FtsK, one of the longest membrane proteins in *E. coli* (1329 amino acids), belongs to the AAA ATPase family, while LolC functions as the membrane domain of the ABC subunit LolD (Sharma et al., 2021). The co-stabilization of LolCD at 61°C showcasing the potential for MM-TPP to capture and stabilizes complexes, providing important details on ligand and protein-protein interactions. In contrast, DgkA, a diacylglycerol kinase and the smallest known membrane kinase in the *E. coli* proteome (122 amino acids) displayed destabilization under the same experimental conditions (Figure 2D) (Li et al., 2015; Zheng and Jia, 2013). Apart from IMPs, we see the stabilization of soluble ATP-binding proteins as well. Collectively, these results validate MM-TPP as a method to identify ATP binders without detergent.

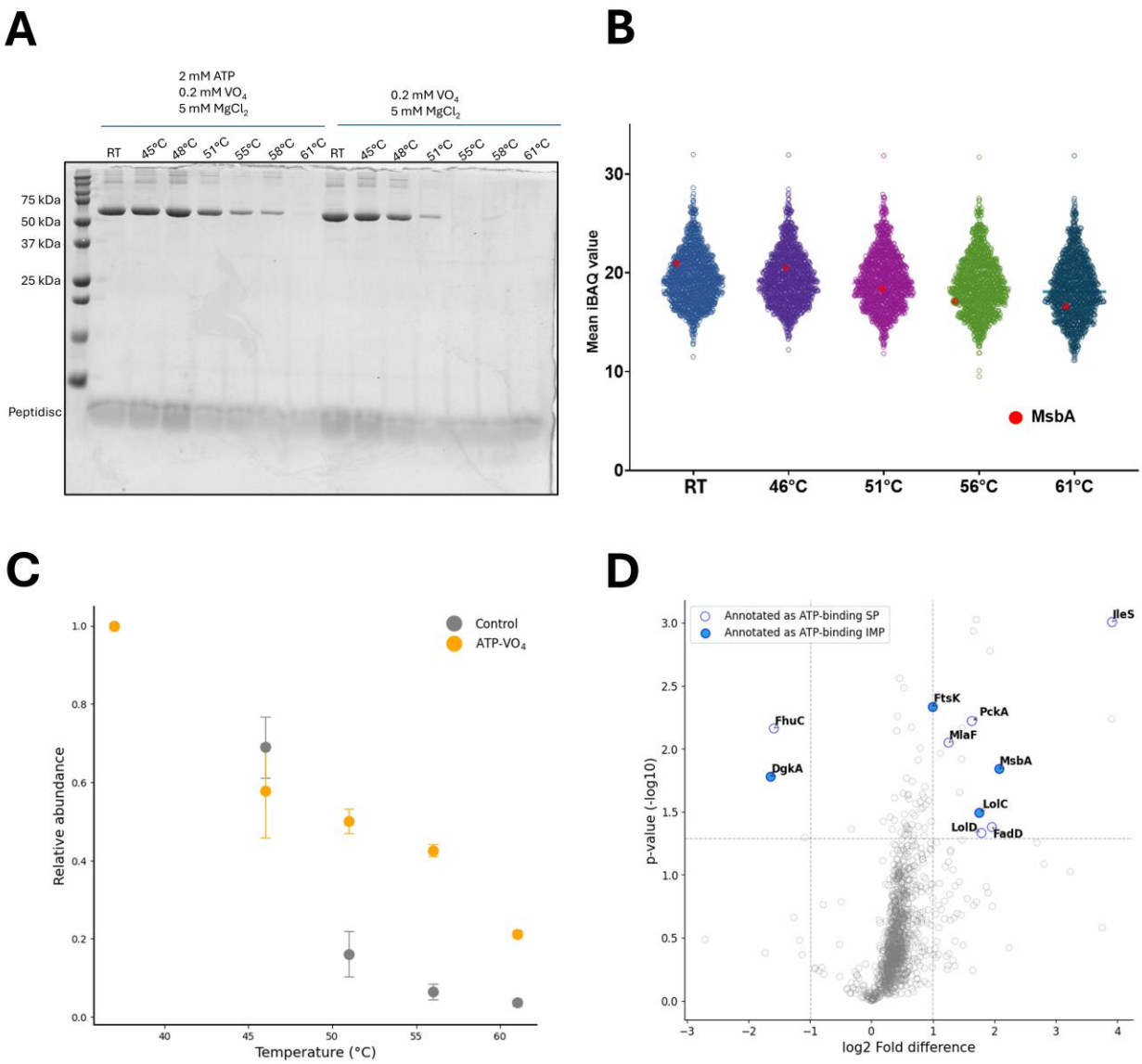

Figure 2: MM-TPP of integral membrane proteins (IMPs) prepared from *E. coli*.

(**A**) Stability of purified MsbA in Peptidisc in the presence of the indicated ligands. Samples are heat treated and centrifuged before analysis by 12% SDS-PAGE and Coomassie blue staining. (**B**) Grouped scatterplot representation of mean IBAQ value obtained for all identified proteins in the *E. coli* library at the indicated temperatures. The location of MsbA on the plot is shown as a red dot. The mean value is obtained from three replicates of the temperature exposure assay (n = 3). (**C**) Relative abundance of MsbA based on the peptide intensities obtained across

temperatures in the presence of ATP-VO_4 (orange) compared to a control sample (gray). Data is a mean ± standard deviation from triplicate assays (n = 3). **(D)** Volcano plot analysis of stabilized and destabilized proteins following ATP-VO_4 exposure at 61°C. A fold difference significance cut off of +2 and -2 with a p-value cutoff of $p \leq 0.05$ is applied. Hollow blue dots indicate ATP-binding soluble proteins (SP) and solid blue dots indicate ATP-binding IMPs. Data represents the mean from three replicates (n = 3).

3.2 Profiling altered lipidic states through MsbA

We isolated the lipids bound to MsbA using three different methods, detergent direct-capture DDC, detergent low-wash (DLW), and detergent high-wash (DHW) (Figure 3A). In all methods, the membrane fraction bearing His6-tagged MsbA was first solubilized with the non-ionic detergent DDM, and the detergent-resistant aggregates were removed by ultra-centrifugation. The membrane detergent extract was then processed in three different ways. In the DDC method, MsbA was reconstituted in peptidisc by detergent dilution and ultra-filtration, followed by purification via IMAC chromatography (DDC-MsbA). In the DLW method, MsbA was purified via standard IMAC chromatography before reconstitution in peptidisc (DLW-MsbA). In the DHW method, MsbA was purified via IMAC chromatography but washed extensively with the detergent buffer (100 column volumes) before reconstitution (DHW-MsbA). As a control, MsbA was purified and eluted in the detergent buffer only (DDM-MsbA). Each preparation was analyzed by SDS-PAGE (Figure 3B). Visual inspection of the gel confirms that MsbA is isolated with comparable purity and yield across the preparations. Inspection of the bottom part of the gel also shows that the number of peptidisc peptides bound to MsbA is relatively similar. The same peptidisc-MsbA preparations were also analyzed by blue native gel

electrophoresis (Figure 3C). On this type of gel, the peptidisc-MsbA particles migrate at slightly different positions depending on the method, probably due to dissimilarity in their lipid content. Overall, the protein migrations are consistent with the homo-dimeric structure of MsbA. We note however that additional bands are detected in the case of DDC-MsbA preparation. Given the high-purity of the preparation (Figure 3B), these bands correspond to higher-order MsbA oligomers.

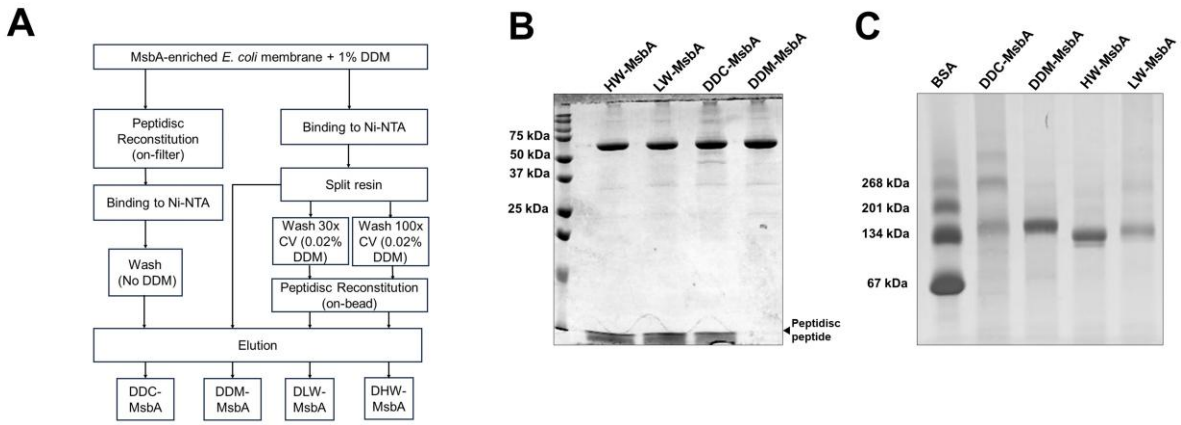

Figure 3: Capture of the MsbA lipidic state. (A) General workflow for purifying MsbA in detergent (DDM-MsbA) or reconstituted peptidiscs via detergent direct capture (DDC-MsbA), detergent low wash (DLW-MsbA), and detergent high wash (DHW-MsbA) methods. The volume of the washing step is indicated in column volume (CV). **(B)** 15% SDS-PAGE analysis of the MsbA preparations followed by Coomassie blue staining of the gel. **(C)** 5–13% clear-native-PAGE analysis of the MsbA preparations followed by Coomassie blue staining. A reference protein ladder is loaded on the left lane on each gel.

3.2.1 Effects of lipids on Peptidisc-MsbA ATPase activity and protein stability

We determined the ATPase activity of the Peptidisc-MsbA preparations, using the DDM-MsbA preparation as a reference. The measurement was performed at 37°C over a period of 10 min (Figure 4A) to estimate the initial rate of ATP hydrolysis (Figure 4B). In agreement with earlier reports, the ATPase activity of DDM-MsbA is 160 nmol/mg/min.32 The ATPase activity of the Peptidisc-MsbA is however 2- to 5-fold higher than in detergent, with the activity increasing from DDC-MsbA to DLW-MsbA to DHW-MsbA. Thus, it appears that the delipidation of MsbA prior to peptidisc reconstitution is correlated with an overall increase in its endogenous ATPase activity.

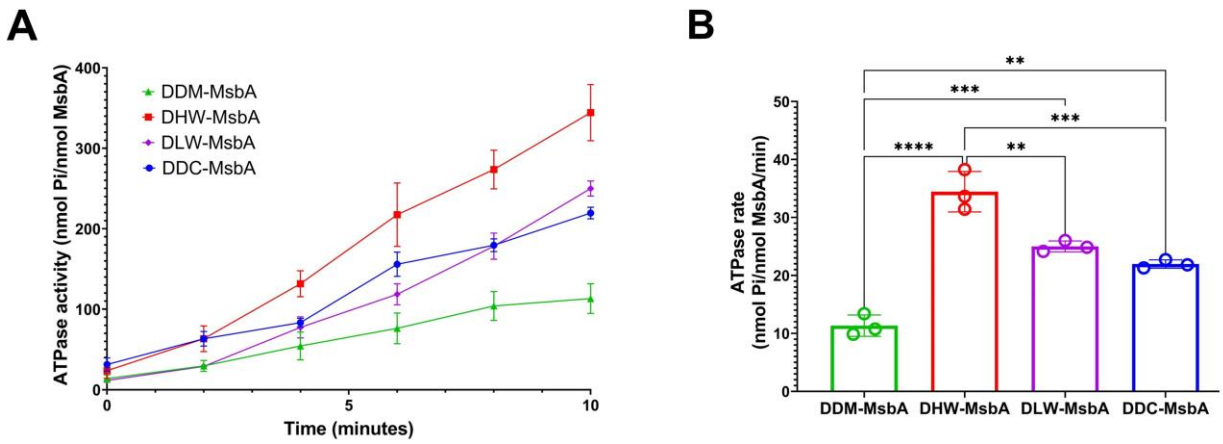

Figure 4: ATPase activity of the DDM-MsbA and Peptidisc-MsbA preparations. (A) The ATPase activity of 5mg of peptidisc reconstituted and DDM solubilized MsbA measured in a Malachite green assay as described in the method details. **(B)** The rate of ATP hydrolysis was quantified for each MsbA sample over a 10 min period. The measured values are presented as mean ± SD (n = 3). Statistical analysis performed by one-way ANOVA with Tukey's multiple comparison test comparing each group, ****$p < 0.0001$, ***$p < 0.001$, **$p < 0.01$.

We determined the stability of the Peptidisc-MsbA preparations using thermal denaturation. Protein aliquots were incubated at 50°C, followed by ultra-centrifugation and SDS-PAGE analysis to estimate the percentage remaining in the soluble fraction. A representative SDS-PAGE dataset, and corresponding triplicate analysis, are presented in Figures 5A and 5B, respectively. The results reveal the low thermal stability of the DDM-MsbA sample, which is consistent with its low ATPase activity (Figure 4). Comparatively, the thermal stability of the Peptidisc-MsbA preparations is much higher (40%–80% higher than detergent), with the stability increasing from DHW-MsbA to DLW-MsbA to DDC-MsbA. Thus, it appears that the higher amount of lipids in the peptidisc preparation confers to the protein a higher thermal stability.

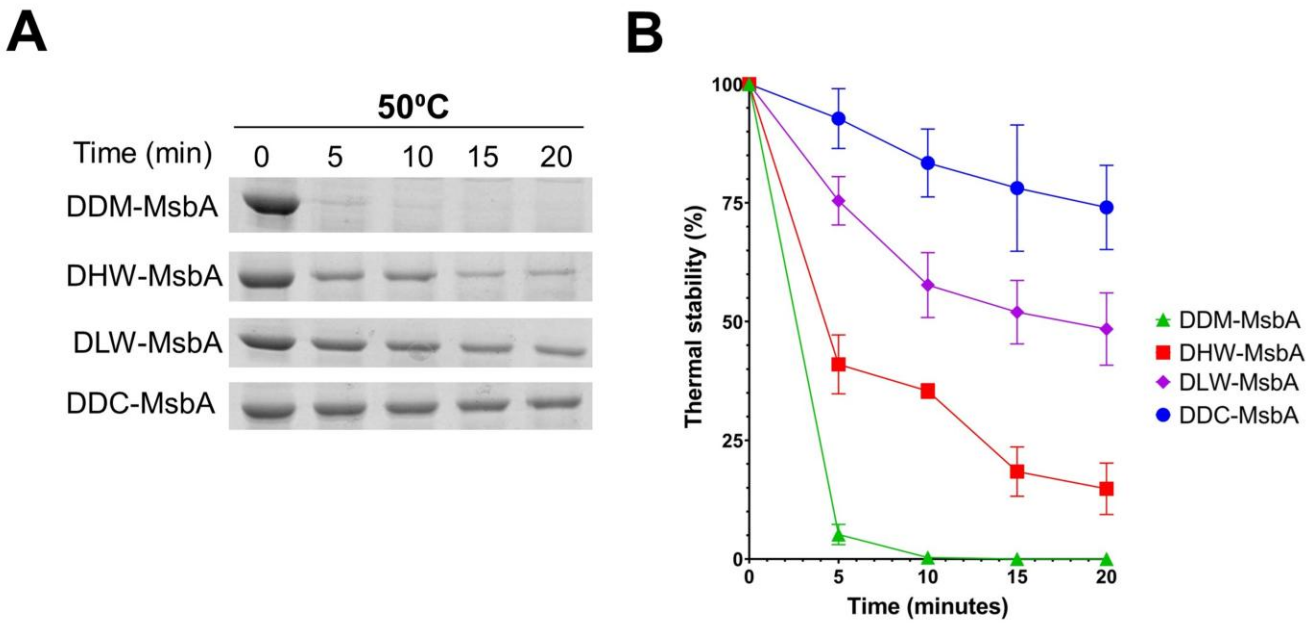

Figure 5: Thermal stability of the DDM-MsbA and Peptidisc-MsbA preparations. (A) The preparations (20 mg each) were incubated at 50°C for the indicated time followed by ultracentrifugation at 180000g along with the room temperature control sample to isolate the thermostable fraction. An aliquot (15 mL) was analyzed by 15% SDS-PAGE and Coomassie

blue staining. The SDS-PAGE is shown as a representative assay. **(B)** The thermal stability assay was performed in triplicate. The intensity of the MsbA protein bands seen on the SDS-PAGE gels were quantified using the ImageJ software and plotted as a linear time course. All values are presented as mean ± SD (n = 3).

3.3 Targeting of the *Mus musculus* liver membrane proteome

We next applied the MM-TPP workflow to the liver organ, where drug screening for cell surface IMPs is particularly relevant. As anticipated, the total number of proteins identified decreased following heat treatment (Figure 6A). Notably, given the absence of detergent, this reduction affected equally soluble proteins and membrane proteins, with the proportion of IMPs remaining stable across temperatures, roughly 48% (Supplementary Table 1). We then conducted MM-TPP in the presence of ATP-VO4 (Figure 6B). Similar to findings obtained with the E. coli library, the majority of proteins displayed increased thermal stability upon ATP-VO4 treatment, as indicated by the rightward shift of the datapoints of the plot. Recent studies show that ATP can act as a natural hydrotrope, influencing the global stability of protein populations by interacting with regions sensitive to thermal fluctuations (Ou et al., 2021; Patel et al., 2017). Important to this study, the GO-term analysis of the significantly stabilized IMPs in the presence of ATP-VO4 revealed enrichment in functions related to nucleoside-phosphate binding and primary active transport (Figure 6C). Accordingly, inspection of the thermal stability profiles obtained at different temperatures confirmed the sensitivity of ABC transporters. Specifically, among the ten ABC transporters identified in the liver library, eight demonstrated significant ATP-VO4 thermal stabilization under at least one temperature condition (Table 1 and Figure 6D).

Table 1: ATP-binding cassette transporters detected in the mouse liver peptidisc library. At least two unique peptides were detected per protein at each temperature. Stabilization was defined using a fold change > 2 between treatment and control samples, with a significance set at $p \leq 0.05$, calculated from triplicate samples (n = 3).

Uniprot-ID	Protein Name	Full protein name	Stabilized temperatures (°C)
Q8K441	ABCA6	ATP-binding cassette sub-family A member 6	51, 56, 60, 64
J3QNY6	ABCB11	ATP-binding cassette, sub-family B (MDR/TAP), member 11	51, 56, 60
Q9DC29	ABCB6	ATP-binding cassette sub-family B (MDR/TAP), member 6	51
Q8VI47	ABCC2	ATP-binding cassette sub-family C (CFTR/MRP), member 2	51, 56, 60
A0A0R4J015	ABCC3	ABC-type glutathione-S-conjugate transporter (CFTR/MRP)	51, 60
P70170	ABCC9	ATP-binding cassette sub-family C member 9 (Sulfonylurea receptor 2)	51, 56, 60
S4R2E1	ABCG2	ATP-binding cassette sub-family G member 2) (Urate exporter)	56, 60, 64
Q99PE8	ABCG5	ATP-binding cassette sub-family G member 5 (Sterolin-1)	51

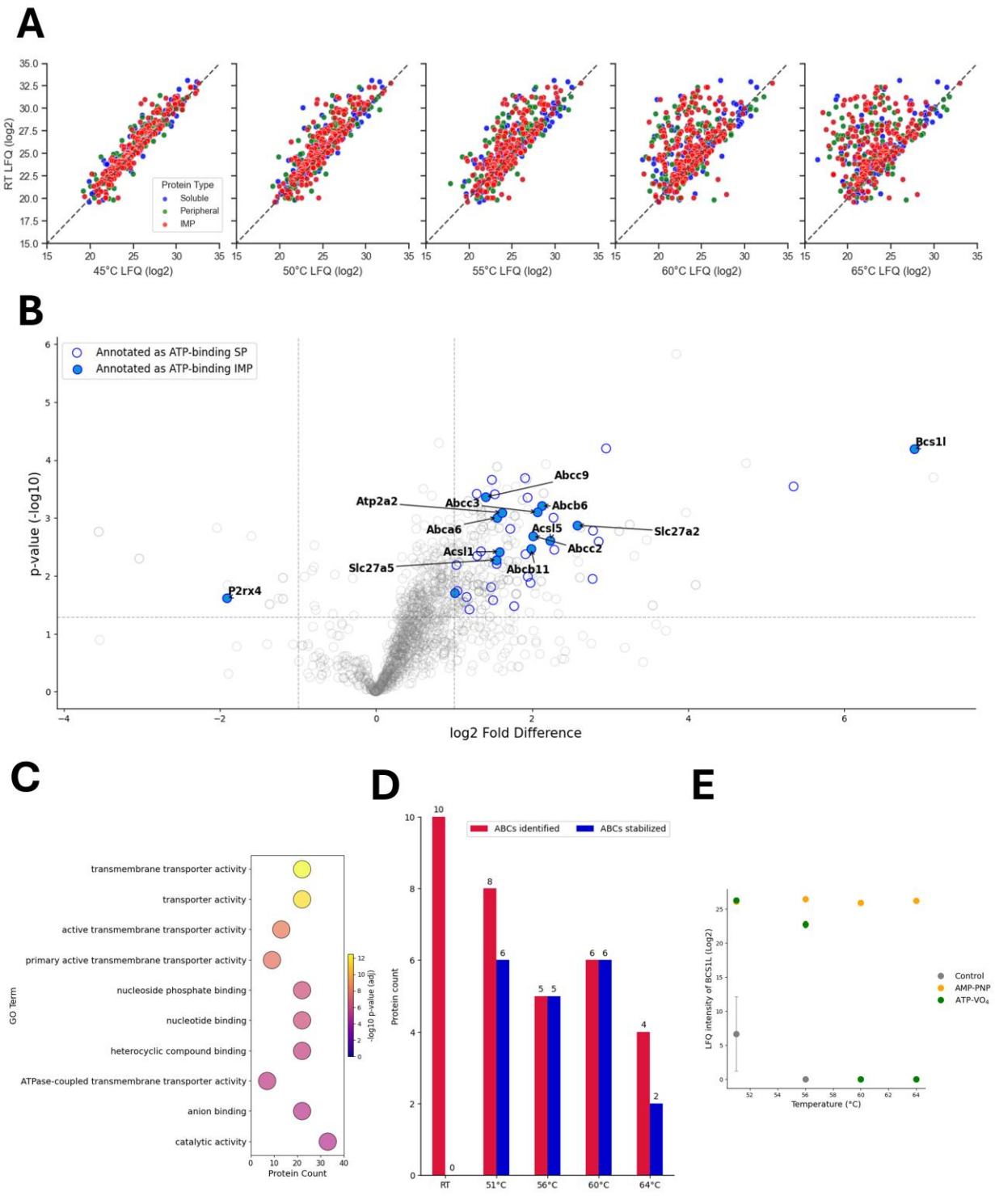

Figure 6: MM-TPP of integral membrane proteins (IMPs) prepared from the mouse liver organ. (**A**) Global protein intensities derived from label-free quantification (LFQ) values of

peptidisc-reconstituted liver extract. The plot displays soluble proteins, peripherally bound and IMPs identified at the indicated temperatures compared to room temperature (RT). The dashed line is the identical value line. (**B**) Volcano plot of stabilized and destabilized proteins at 51°C based on a fold difference cutoff of > 2 or < -2 and p-value of ≤ 0.05. The ATP-binding soluble proteins (SP) are represented as hollow blue circles, and the ATP-binding IMPs are represented as solid blue circles. The mean value is obtained from three replicates at the temperature exposure assay (n = 3). (**C**) GO-term enrichment analysis of molecular functions of stabilized IMPs identified in B. The presented top 10 significant terms are based on adjusted p-value (FDR = 5% after Benjamini-Hochberg correction) (**D**) Number of ATP-binding cassette (ABC) transporters identified and stabilized by ATP-VO_4 at the indicated temperatures. (**E**) Peptide intensities (LFQ) of BCS1L in the presence of ATP-VO_4 (green), AMP-PNP (orange), and vehicle control (gray) across the temperature range. Data is a mean ± standard deviation from three replicates (n = 3).

Prominent ABC transporters of the liver are demonstrated to showcase multi-temperature stabilization such as the BSEP transporter ABCB11, the multi-drug resistance ABCC2, and the sulfonylurea receptor ABCC9, which plays a crucial role in glucose metabolism. Besides ABC transporters, the BCS1L protein exhibited a remarkable ~30-fold increase in stability, which was further enhanced in the presence of AMP-PNP (Figure 6E and Supplementary Figure 2). Interestingly, BCS1L demonstrates one of the largest significant fold-changes in our protein libraries in the presence of both ATP-VO_4 and AMP-PNP across all tested temperatures and was not detected in the absence of these ligands. This heightened stability aligns with the recent structural analyses showing that the heptameric BCS1L complex undergoes substantial

conformational changes upon binding of this non-hydrolyzable ATP analog (Pan et al., 2023; Tang et al., 2020; Zhan et al., 2024). Given the abundance of SLC transporters present within the liver, our data set identifies the stabilization of this protein family as well. Notably, two long-chain fatty acid transporters FATP2/SLC27A2 and FATP5/SLC27A5 are known ATP-binding IMPs that remained significantly stabilized at all tested temperatures (Figure 7). In totality, 17 unique membrane-bound SLC transporters were stabilized across all tested temperatures.

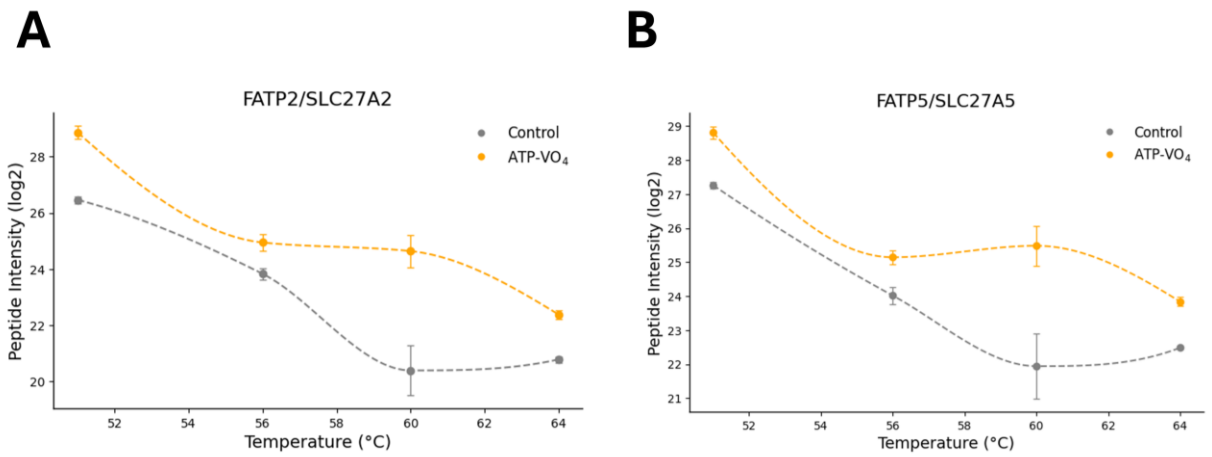

Figure 7: Thermal stabilization of SLC transporters with ATP-VO_4. (**A**) Peptide intensities (LFQ) of FATP2/SLC27A2 in the presence of ATP-VO_4 (orange) and vehicle control (gray) across the temperature range. Data is a mean ± standard deviation from three replicates (n = 3). (**B**) Peptide intensities of FATP5/SLC27A5 in the presence of ATP-VO_4 (orange) and vehicle control (gray) across the temperature range. Data is a mean ± standard deviation from three replicates (n = 3).

3.4 On & off-protein targeting through ATP dynamics

A large proportion of IMPs without an ATP-binding annotation were also identified as significantly stabilized in the presence of ATP-VO4. For example, out of the 178 IMPs above the

cut-off significance value, ~ 43% were annotated with GO terms such as nucleic acid/nucleotide, GTP and phosphate binders, among others (Figure 8A). Some IMPs may achieve stability through interactions with ATP-binding proteins, indirectly enhancing their structural stability, as is the case for the LolC/LolD, mentioned in section 3.2. Conversely, other IMPs may gain stability due to an off-target ligand effect, for example, when metabolized ATP products like ADP, AMP or Pi improve protein stability. This scenario could apply to the purinergic receptor P2RY6, a GPCR responsive to ADP rather than ATP (von Kügelgen and Hoffmann, 2016). This protein displays the highest gain in thermal stability among the other IMPs detected at 56°C. Similarly, P2RY12, a member of the same GPCR family, showed significant stabilization at all tested temperatures despite its preference for ADP (Entsie et al., 2023; Zhang et al., 2014). In support of this, no such thermal stability gain was obtained when these two receptors were exposed to the ATP analog AMP-PNP (Figure 8B). Conversely, the trimeric ATP-gated cation channel P2RX4 exhibited significant destabilization in the presence of ATP-VO4 (Figure 6B) or AMP-PNP (Figure 8C), in agreement with literature reports indicating that members of the P2RX family differ from P2RY due to their preference for ATP (Carnero Corrales et al., 2021; Thompson et al., 2021). Most strikingly, the greatest gain in ATP-induced thermal stability was observed with the FAD-containing monoamine oxidase Mao-B protein at 64°C (Supplementary Figure 3). To identify the potential reason for this major off-target effect, we utilized AlphaFold3 to model ATP and its derivatives within the FAD-binding pocket of Mao-B (Abramson et al., 2024). Notably, the best fit obtained was for ADP and AMP, with a Predicted Local Distance Difference Test (pLDDT) value greater than 90, while ATP generated the lowest pLDDT score (Figure 8D). Collectively, these data highlight the ability of MM-TPP to detect the side effects of parent compounds, an important consideration for drug development.

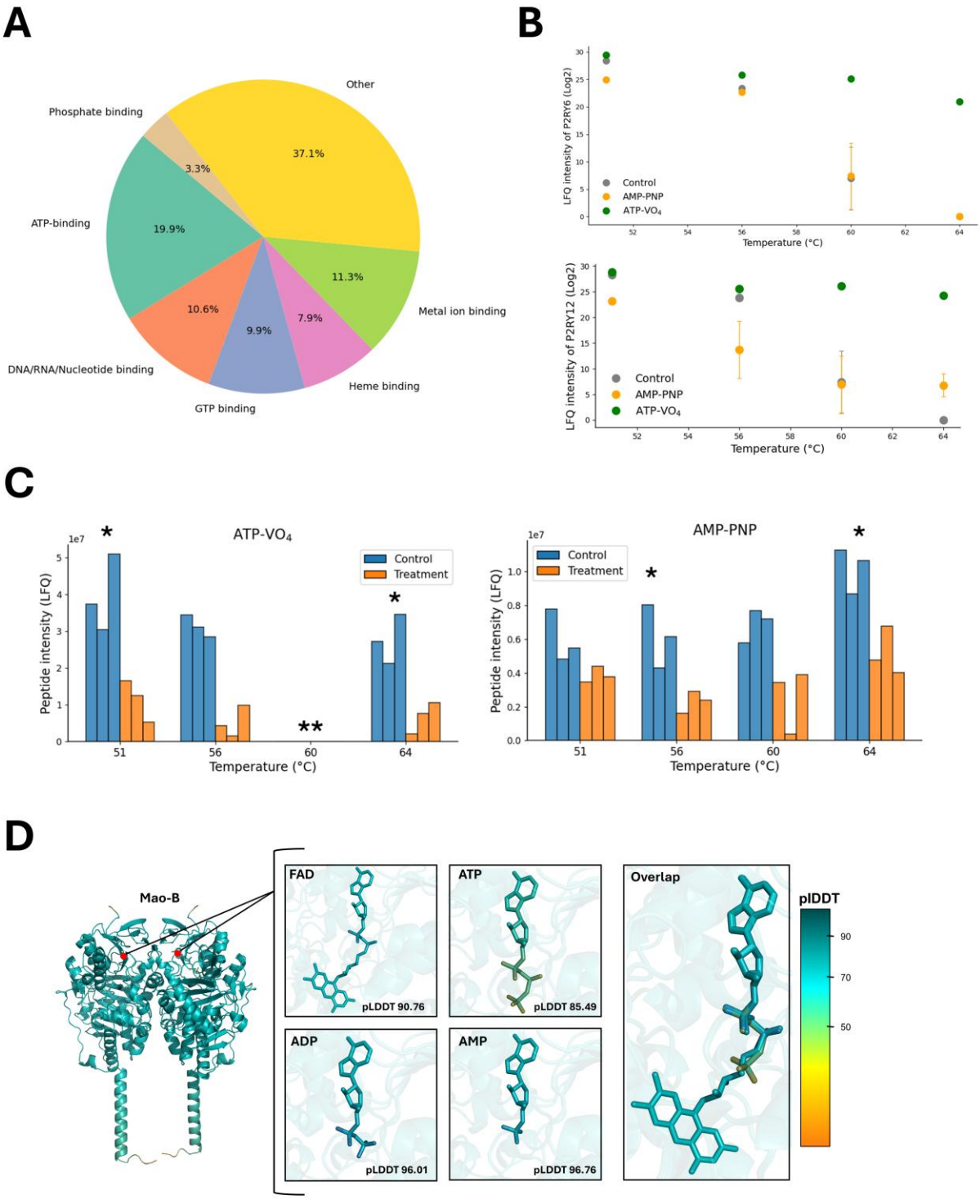

Figure 8: Off-target ATP ligand effect. (**A**) GO-term analysis of molecular functions and distribution for all IMPs significantly stabilized at all temperatures tested with the mouse liver

library (n = 178). (**B**) Peptide intensity (LFQ) variations of P2RY6 and P2RY12 over the temperature range with AMP-PNP (orange), ATP-VO_4 (green), or none (gray). Data is a mean ± standard deviation from three replicates (n = 3). **(C)** Peptide intensity variations of P2RX4 at the indicated temperature in the presence of ATP-VO4 (left panel) or AMP-PNP (right panel). Data from treatment samples (orange) and control samples (blue) is from triplicates (n = 3). * Represents p-value ≤ 0.05. **Protein not detected. (**D**) Structural model of homodimeric Mao-B with the predicted binding of FAD, ATP, ADP, and AMP ligands within the FAD binding pocket, indicated as red dots. Each ligand is presented individually in the FAD binding pocket or as an all-ligand overlap generated by *AlphaFold3*. The respective Predicted Local Distance Difference Test (pLDDT) score for each ligand is shown, with higher scores representing more favourable ligand fitting. The colour gradient represents a high pLDDT score as blue and a low pLDDT score as orange.

3.5 Comparison of MM-TPP to a detergent-based TPP assay

To further evaluate the effectiveness of MM-TPP, we compared its ability to assess membrane protein stability upon ligand binding to a detergent-based TPP assay (DB-TPP). Crude membrane fractions extracted from mouse liver were solubilized in 1% DDM to extract MPs. These samples underwent the same treatment conditions as MM-TPP, with the addition of a detergent removal step prior to MS analysis. Notably, DB-TPP provides broader coverage of the membrane proteome, identifying a greater number of total proteins, including ATP-binding proteins (Table 2).

Table 2: Comparison of MM-TPP and DB-TPP. Number of identified and stabilized proteins at each tested temperature condition after downstream data analysis. **(A)** MM-TPP in the presence of ATP-VO_4 and **(B)** DB-TPP in the presence of ATP-VO_4. The values represent the total number of proteins that met the inclusion criteria based on triplicate control and treatment conditions. Since protein counts are determined post-analysis, they are reported as single values rather than means with standard deviations. At least two unique peptides were identified for each protein (n = 3).

A

	Total protein	Total MPs	Total ATP-binding	Total stabilized	Total ATP-binding stabilized	Total MP stabilized	Total ATP-binding MPs	Total ATP-binding MPs stabilized
51°C	1380	419 (30%)	129	301	45	108	37	14
56°C	1179	369 (31%)	107	218	44	64	33	15
60°C	1090	344 (32%)	101	229	31	74	31	15
64°C	992	316 (32%)	80	336	41	117	31	18

B

	Total protein	Total MPs	Total ATP-binding	Total stabilized	Total ATP-binding stabilized	Total MP stabilized	Total ATP-binding MPs	Total ATP-binding MPs stabilized
51°C	3097	773 (25%)	260	43	15	6	48	2
56°C	3009	765 (25%)	261	77	17	6	43	4
60°C	2651	676 (25%)	191	144	15	27	33	3
64°C	2481	628 (25%)	183	47	8	47	35	0

However, this increased coverage comes at a cost of a higher proportion of soluble proteins. By contrast, MM-TPP generates a more MP-enriched library due to the reduced

presence of soluble proteins following peptidisc reconstitution. More importantly, while DB-TPP captures more proteins overall, it lacks the sensitivity to detect the stabilization of ATP-binding MPs upon ATP-VO_4 exposure. At the tested temperatures, DB-TPP identifies an average of 2 significantly stabilized MP-ATP, whereas MM-TPP detects 15. This is most apparent at the highest temperature condition of 64°C, where no ATP-binding MP was significantly stabilized in DB-TPP (Table 2). Among the few ATP-binding MPs stabilized in DB-TPP, some overlap with MM-TPP is observed, as demonstrated by the stabilization of BCS1L at 51°C (Figure 9). However, BCS1L was not identified at any other temperature condition in DB-TPP, in contrast to its consistently strong stabilization across multiple temperatures in MM-TPP.

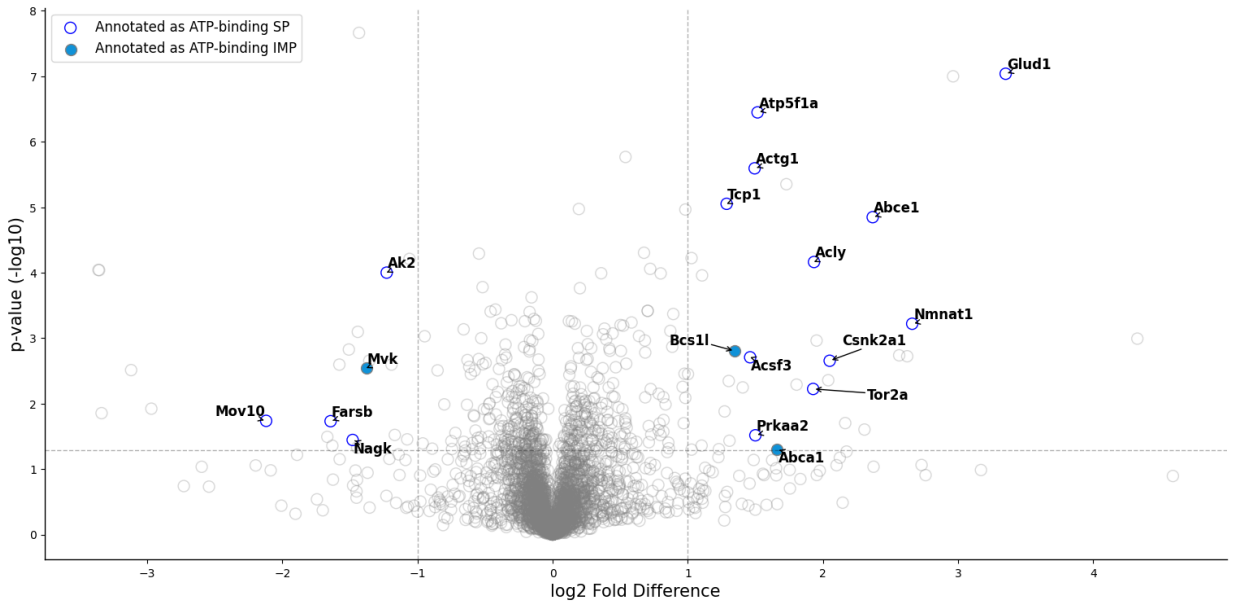

Figure 9: Volcano plot of stabilized and destabilized proteins at 51°C in the presence of ATP-VO_4 in detergent-based TPP. Volcano plot of stabilized and destabilized proteins at 51°C based on a fold difference cutoff of > 2 or < -2 and p-value of ≤ 0.05. The ATP-binding soluble proteins (SP) are represented as hollow blue circles, and the ATP-binding IMPs are represented as solid blue circles. The mean value is obtained from three replicates (n = 3).

Chapter 4: Discussion

4.1 MM-TPP towards mapping membrane protein-ligand dynamics

Thermal proteome profiling (TPP) has become a widely adopted method for studying protein-ligand interactions, drug target engagement, and proteome-wide stability changes (Savitski et al., 2014). Since its introduction, multiple refinements have improved its sensitivity and scope, including mild detergent use to expand TPP to membrane proteins (Huber et al., 2015; Reinhard et al., 2015), the development of 2D-TPP for deeper stability profiling (Becher et al., 2016), and the optimization of lysis and fractionation protocols for broader organism compatibility (Mateus et al., 2018; Perrin et al., 2020). While these advancements have made TPP more versatile, they have also introduced new challenges, particularly in membrane protein (MP) characterization. One of these limitations in TPP has been the reliance on detergent-solubilized environments for membrane proteome coverage. Although detergents increase MP extraction efficiency, they disrupt native protein-protein and protein-lipid interactions, leading to altered stability profiles that may not reflect true biological conditions. Moreover, the effect of detergents on protein target identification remains debated—while some studies report increased MP detection, others show reduced target sensitivity (Berlin et al., 2023; Reinhard et al., 2015; Ye et al., 2023).

To address these challenges, we introduce MM-TPP, an approach that keeps functionally active and water-soluble MPs in a detergent-free environment. Using peptidisc libraries derived from *E. coli* and mouse liver membranes, we identified a diverse range of ATP-binding MPs. Additionally, MM-TPP revealed co-stabilization of non-ATP nucleotide binders, suggesting its potential for detecting downstream metabolic effects of ligand exposure. Collectively, MM-TPP

offers an alternative to traditional TPP, enabling membrane proteome analysis without the confounding effects of detergents.

Previous attempts to analyze ATP's influence on proteomes in detergent-solubilized environments have often been limited in scope. For example, a previous study using NP-40 solubilized K562 lysates identified three ABC transporters with significant ATP-dependent changes in melting temperature (Reinhard et al., 2015). The partnering of ATP with VO_4 has consistently been shown to bind and inhibit the transporter activity of ABC transporters *in-vivo*, when purified in detergent, as well as when reconstituted in membrane mimetics (Angiulli et al., 2020; Behrens et al., 2019; Pytkowski & Jagodzińska-Hamann, 1996; Sharma et al., 2021). Through MM-TPP, we leveraged this dual-ligand exposure to identify three-fold more ABC transporters with significant ATP-dependent changes in thermal stability compared to this previous study (Reinhard et al., 2015). These include those previously validated to be inhibited by ATP-VO_4, such as the primary hepatocyte bile acid salt transport ABCB11 (H. Liu et al., 2023) and the breast cancer resistance protein ABCG2 (Khunweeraphong et al., 2017; Taylor et al., 2017). Our data confirms the known stabilization of BCS1L, a heptameric inner mitochondrial membrane protein involved in the transport of folded iron-sulfur protein (Reinhard et al., 2015). MM-TPP further highlights its ligand-specific preference for stability, showing strong stabilization under the nonhydrolyzable AMP-PNP compared to ATP-VO_4. Notably, BCS1L displayed stronger stabilization under non-hydrolysable AMP-PNP than ATP-VO_4, consistent with structural analyses suggesting AMP-PNP induces conformational stabilization in heptameric state (Pan et al., 2023; Tang et al., 2020; Zhan et al., 2024). These findings demonstrate MM-TPP's ability to detect subtle, ligand-specific stabilization mechanisms more effectively in detergent-free environments.

Through removing detergents, MM-TPP offers a sensitive environment that discerns the broad effects of ATP exposure. Upon ATP-VO_4 treatment, *E. coli* and mouse liver libraries displayed increased thermal stability as indicated by the rightward shift of data-points. As a natural hydrotrope, ATP sequesters around thermally sensitive regions and regions of high hydrophobicity, potentially shielding proteins from denaturing stress (Patel et al., 2017). This in-turn, may promote global protein stability (Ou et al., 2021; Patel et al., 2017). The propensity for ATP to stabilize non-ATP binders was highlighted in MM-TPP, mainly amongst proteins annotated as GTP or other nucleotide binders. This is similar to previous system-wide studies in *E. coli* and Jurkat cell lysates (Piazza et al., 2018; Sridharan et al., 2019). Consistent with these studies, a notable portion of ATP-influenced proteins are not annotated in Uniprot as ATP binders, suggesting certain ATP concentrations promote stabilization of diverse macromolecule-binding proteins, including those associated with NAD, FAD, NTPs, DNA, RNA, and their regulatory complexes (Sridharan et al., 2019). ATP hydrolysis by-products may also indirectly influence downstream stabilization of key membrane protein classes such as ion channels and GPCRs – membrane protein classes that make up the largest targets of current approved pharmaceuticals (Rosenbaum et al., 2020; D. Yang et al., 2021). As functional proteins increase the concentration of ADP, AMP, and free phosphate in the system, these molecules can contribute to the observed stabilizations of non-ATP annotated proteins. As more researchers rely on AlphaFold3 to further confirm these binding events, MM-TPP enables large-scale production of experimentally validated data on ligand binding, providing a rich reservoir of data necessary to train and enhance next-generation computational tools (Mullowney et al., 2023; Siebenmorgen et al., 2024).

Collectively, MM-TPP is useful in characterizing membrane proteomes in a detergent-free context, with potentially broad applications in proteomics and drug discovery. By enabling large-scale detection of ligand interactions, MM-TPP holds promise for exploring complex, tissue-specific proteomes and facilitating targeted drug design. Future adaptations to MM-TPP will further expand its utility, driving novel insights into membrane protein biology and therapeutic targeting across diverse ligand classes and membrane environments.

4.2 Capture of endogenous lipids in peptidisc & effect on protein stability & activity

During MP purification, prolonged exposure to the detergent micelles progressively strips away bound lipids, a process known as delipidation (Bechara et al., 2015; Gupta et al., 2018). We exploit this property here to isolate MPs containing various amounts of endogenous lipids, and we capture these lipid intermediate states in peptidiscs using three methods. In the detergent direct capture (DDC) method, the target protein is reconstituted immediately after detergent extraction to maximize the chance of capturing its naturally bound lipids. In the detergent low wash and high wash methods (DLW and DHW), the protein is exposed to increasing amounts of detergent to maximize its delipidation before reconstitution. These workflows allow us to assess the impact of endogenous lipids on protein stability and activity. With the ABC transporter MsbA, the DDC method allows to capture ~10 times more PE and PG lipids than with the DHW method (Jandu et al., 2024).

As a direct consequence, the thermal stability of MsbA is dramatically increased, with ~75% of the DDC-MsbA remaining soluble after a 20-min incubation at 50°C compared to only ~15% when MsbA is delipidated (Figure 5). The lipidomic analysis further showed that the different PE and PG lipid classes were equally depleted during the detergent treatment,

suggesting that MsbA does not have particular lipid specificity (Jandu et al., 2024). The lipid-mediated increased thermal stability we report is a significant finding because it indicates that the capture of MPs directly from the initial lipid-detergent extract, before purification, is an effective way to increase protein stability and thereby the protein downstream usability. The presence of endogenous lipids increased the thermal stability of MsbA, yet these additional lipids also lowered the transporter ATPase activity. It is well known that MsbA ATPase depends on the closure of its two nucleotide-binding domains which is coupled to the opening of its two transmembrane domains, termed the outward-facing (OF) conformation (Ward et al., 2007).

Previous work showed that delipidated MsbA in peptidisc is stabilized in this OF conformation, which is consistent with the higher ATPase activity obtained with this sample (Angiulli et al., 2020). We therefore predict here that the high lipid content of the DDC-MsbA preparation lowers the MsbA ATPase activity because lipids stabilize the transporter in the inward-facing (IF) conformation. This assumption seems supported by a recent structural analysis conducted in E. coli showing that MsbA exists mostly in the IF conformation when embedded in the native membrane environment (Galazzo et al., 2022). While it is unlikely that the natural lipid bilayer constraint is reconstituted in peptidisc, the current result clearly shows that the MsbA activity is directly influenced by the lipid environment. Finally, we note that MsbA is often overproduced in the membrane before purification, and the consequence of this overproduction on protein-lipid associations is unknown. Specifically, our native-gel analysis shows that protein oligomers are captured when MsbA is purified using the DDC method (Figure 3C). These oligomers were also obtained when overproduced MsbA was extracted from the membrane using the SMA polymer (Pollock et al., 2022), indicating the tendency of this protein to cluster together in the membrane environment.

4.3 Limitations & future directions

In this work, we have demonstrated that MP reconstitution using peptidisc can significantly influence protein activity and stability. Specifically, the methods of detergent direct capture (DDC), direct light wash (DLW), and detergent high wash (DHW) modulate the lipid environment surrounding the captured proteins. These changes in lipid composition play a critical role in protein stabilization, as evidenced by the observed lipid-mediated increase in the thermal stability of MsbA. However, further studies are required to quantify the exact number of lipid molecules bound to MsbA under each preparation condition. Understanding the precise lipid composition of these reconstituted proteins will provide critical insights into their activity and how these interactions contribute to stability. Additionally, this information could guide the optimization of peptidisc-based workflows for stabilizing IMPs.

Despite its advantages, this approach still requires an initial detergent solubilization step to extract MPs from purified crude membranes. While detergent solubilization enhances MP extraction efficiency (Perrin et al., 2020), it risks disrupting native protein-protein and protein-lipid interactions, potentially removing biologically relevant lipids. In contrast, detergent-free approaches, such as styrene-maleic acid-lipid particles (SMALPs), have shown comparable MP solubilization efficiency (Brown et al., 2024). While SMA copolymers can assess protein functionality in isolated protein studies (Bada Juarez et al., 2020; Cherepanov et al., 2019); its application in whole-proteome ligand exposure remains unexplored.

An additional limitation in the current work is the indirect inference of protein stability through the presence of metabolized products, such as ADP generated by ATP hydrolysis.

Although this finding supports the role of ligand-metabolism products in protein stabilization, incorporating a direct measurement of ligand binding and stability would strengthen the conclusion. Also, as traditional TPP experiments have been focused on small-molecule exposure, venturing towards different families of druggable ligands will be beneficial. A favourable direction is towards the testing of biologics, such as antibodies or peptide-based hormones, building off of previous protein-protein interaction models of TPP (Mateus et al., 2020; Searle, 2024).

Another area for improvement is the number of temperature points tested during thermal proteome profiling. A limited number of conditions restricts the resolution of protein melting behavior, affecting precise stability assessments across tissue- and organ-specific proteomes. Increasing temperature sampling points would enable higher-resolution profiling and improve accuracy in defining melting temperatures. Additionally, conclusions made from MM-TPP analysis could be enhanced through orthogonal experiments, such as overexpression and targeted mutagenesis, to confirm findings and validate interactions.

With the success of establishing MM-TPP, this methodology can potentially be utilized in large scale drug discovery methods, as is presented through affinity-selection mass spectrometry (AS-MS) (Muchiri & van Breemen, 2021). By generating peptidisc libraries of MPs, we can screen many IMPs against single compounds or a library of compounds for high-throughput analysis of ligand binding. Additionally, peptidisc offers a unique capability for enriching low-abundance MPs through affinity-based capture of the library (Saville et al., 2019; Young et al., 2020). Future efforts to integrate these modified peptidisc peptides into MM-TPP could enable the assessment of crucial, yet low-abundance proteins, such as those located at the

plasma membrane (Z. Zhao et al., 2023). This can be especially beneficial in organ samples, which can be analyzed in their unperturbed and diseased states to obtain an accurate proteome profile for drug exposure (Perrin et al., 2020).

Overall, while this study provides a strong foundation for the use of peptidisc-based MM-TPP workflows, addressing these limitations and incorporating the suggested future directions will significantly enhance the utility of this technique in studying membrane proteomes and their interactions. By refining these methods, we can unlock new opportunities for exploring the role of membrane proteins in cellular physiology and therapeutic development.

4.4 Conclusion

In this thesis, a novel membrane mimetic-based TPP workflow was successfully developed to enable the investigation of ligand binding on whole, functional membrane proteomes in a detergent-free environment. Using ATP as a model ligand, we demonstrated the feasibility of MM-TPP for detecting ligand-specific interactions and elucidating downstream effects of ligand metabolism, including the potential off-target stabilization by metabolic byproducts such as ADP. Furthermore, we extended the scope of MM-TPP to explore non-small-molecule determinants of thermal stability, revealing the critical role of co-captured lipids in modulating protein stability and function. This workflow was validated across both prokaryotic systems, using *E. coli*, and eukaryotic systems, including organ tissues from *M. musculus*, establishing MM-TPP as a versatile and robust approach for advancing membrane proteome characterization and its applications in drug discovery and proteomics.

References

Addis, P., Bali, U., Baron, F., Campbell, A., Harborne, S., Jagger, L., Milne, G., Pearce, M., Rosethorne, E. M., Satchell, R., Swift, D., Young, B., & Unitt, J. F. (2024). Key aspects of modern GPCR drug discovery. *SLAS Discovery*, *29*(1), 1–22. https://doi.org/10.1016/j.slasd.2023.08.007

Aebersold, R., & Mann, M. (2016). Mass-spectrometric exploration of proteome structure and function. *Nature*, *537*(7620), 347–355. https://doi.org/10.1038/nature19949

Alberts, B., Johnson, A., Lewis, J., Morgan, D., Raff, M., Roberts, K., & Walter, P. (2015). *Molecular Biology of the Cell* (Sixth edition, Onkine-Ausgabe). Garland Science.

Angiulli, G., Dhupar, H. S., Suzuki, H., Wason, I. S., Duong Van Hoa, F., & Walz, T. (2020). New approach for membrane protein reconstitution into peptidiscs and basis for their adaptability to different proteins. *eLife*, *9*, e53530. https://doi.org/10.7554/eLife.53530

Antony, F., Brough, Z., Orangi, M., Al-Seragi, M., Aoki, H., Babu, M., & Duong van Hoa, F. (2024). Sensitive Profiling of Mouse Liver Membrane Proteome Dysregulation Following a High-Fat and Alcohol Diet Treatment. *PROTEOMICS*, *n/a*(n/a). https://doi.org/10.1002/pmic.202300599

Antony, F., Brough, Z., Zhao, Z., & Duong van Hoa, F. (2024). Capture of the Mouse Organ Membrane Proteome Specificity in Peptidisc Libraries. *Journal of Proteome Research*, *23*(2), 857–867. https://doi.org/10.1021/acs.jproteome.3c00825

Arachea, B. T., Sun, Z., Potente, N., Malik, R., Isailovic, D., & Viola, R. E. (2012). Detergent selection for enhanced extraction of membrane proteins. *Protein Expression and Purification*, *86*(1), 12–20. https://doi.org/10.1016/j.pep.2012.08.016

Babcock, J. J., & Li, M. (2014). Deorphanizing the human transmembrane genome: A landscape of uncharacterized membrane proteins. *Acta Pharmacologica Sinica*, *35*(1), Article 1. https://doi.org/10.1038/aps.2013.142

Bada Juarez, J. F., Muñoz-García, J. C., Inácio dos Reis, R., Henry, A., McMillan, D., Kriek, M., Wood, M., Vandenplas, C., Sands, Z., Castro, L., Taylor, R., & Watts, A. (2020). Detergent-free extraction of a functional low-expressing GPCR from a human cell line. *Biochimica et Biophysica Acta (BBA) - Biomembranes*, *1862*(3), 183152. https://doi.org/10.1016/j.bbamem.2019.183152

Bantscheff, M., Hopf, C., Savitski, M. M., Dittmann, A., Grandi, P., Michon, A.-M., Schlegl, J., Abraham, Y., Becher, I., Bergamini, G., Boesche, M., Delling, M., Dümpelfeld, B., Eberhard, D., Huthmacher, C., Mathieson, T., Poeckel, D., Reader, V., Strunk, K., … Drewes, G. (2011). Chemoproteomics profiling of HDAC inhibitors reveals selective targeting of HDAC complexes. *Nature Biotechnology*, *29*(3), 255–265. https://doi.org/10.1038/nbt.1759

Barrera, N. P., Zhou, M., & Robinson, C. V. (2013). The role of lipids in defining membrane protein interactions: Insights from mass spectrometry. *Trends in Cell Biology*, *23*(1), 1–8. https://doi.org/10.1016/j.tcb.2012.08.007

Bartels, K., Lasitza-Male, T., Hofmann, H., & Löw, C. (2021). Single-Molecule FRET of Membrane Transport Proteins. *ChemBioChem*, *22*(17), 2657–2671. https://doi.org/10.1002/cbic.202100106

Bayburt, T. H., Grinkova, Y. V., & Sligar, S. G. (2002). Self-Assembly of Discoidal Phospholipid Bilayer Nanoparticles with Membrane Scaffold Proteins. *Nano Letters*, *2*(8), 853–856. https://doi.org/10.1021/nl025623k

Bechara, C., Nöll, A., Morgner, N., Degiacomi, M. T., Tampé, R., & Robinson, C. V. (2015). A subset of annular lipids is linked to the flippase activity of an ABC transporter. *Nature Chemistry*, *7*(3), Article 3. https://doi.org/10.1038/nchem.2172

Becher, I., Savitski, M. M., Savitski, M. F., Hopf, C., Bantscheff, M., & Drewes, G. (2013). Affinity Profiling of the Cellular Kinome for the Nucleotide Cofactors ATP, ADP, and GTP. *ACS Chemical Biology*, *8*(3), 599–607. https://doi.org/10.1021/cb3005879

Becher, I., Werner, T., Doce, C., Zaal, E. A., Tögel, I., Khan, C. A., Rueger, A., Muelbaier, M., Salzer, E., Berkers, C. R., Fitzpatrick, P. F., Bantscheff, M., & Savitski, M. M. (2016). Thermal profiling reveals phenylalanine hydroxylase as an off-target of panobinostat. *Nature Chemical Biology*, *12*(11), 908–910. https://doi.org/10.1038/nchembio.2185

Beck, M., Schmidt, A., Malmstroem, J., Claassen, M., Ori, A., Szymborska, A., Herzog, F., Rinner, O., Ellenberg, J., & Aebersold, R. (2011). The quantitative proteome of a human cell line. *Molecular Systems Biology*, *7*(1), 549. https://doi.org/10.1038/msb.2011.82

Beer, L. A., Liu, P., Ky, B., Barnhart, K. T., & Speicher, D. W. (2017). Efficient quantitative comparisons of plasma proteomes using label-free analysis with MaxQuant. *Methods in Molecular Biology (Clifton, N.J.)*, *1619*, 339–352. https://doi.org/10.1007/978-1-4939-7057-5_23

Behnke, J.-S., & Urner, L. H. (2023). Emergence of mass spectrometry detergents for membrane proteomics. *Analytical and Bioanalytical Chemistry*, *415*(18), 3897–3909. https://doi.org/10.1007/s00216-023-04584-z

Behrens, C. E., Smith, K. E., Iancu, C. V., Choe, J., & Dean, J. V. (2019). Transport of Anthocyanins and other Flavonoids by the Arabidopsis ATP-Binding Cassette

Transporter AtABCC2. *Scientific Reports*, *9*(1), 437. https://doi.org/10.1038/s41598-018-37504-8

Berasain, C., & Avila, M. A. (2014). The EGFR signalling system in the liver: From hepatoprotection to hepatocarcinogenesis. *Journal of Gastroenterology*, *49*(1), 9–23. https://doi.org/10.1007/s00535-013-0907-x

Berlin, E., Lizano-Fallas, V., Carrasco del Amor, A., Fresnedo, O., & Cristobal, S. (2023). Nonionic Surfactants can Modify the Thermal Stability of Globular and Membrane Proteins Interfering with the Thermal Proteome Profiling Principles to Identify Protein Targets. *Analytical Chemistry*, *95*(8), 4033–4042. https://doi.org/10.1021/acs.analchem.2c04500

Blouin, A., Bolender, R. P., & Weibel, E. R. (1977). Distribution of organelles and membranes between hepatocytes and nonhepatocytes in the rat liver parenchyma. A stereological study. *Journal of Cell Biology*, *72*(2), 441–455. https://doi.org/10.1083/jcb.72.2.441

Bolla, J. R., Agasid, M. T., Mehmood, S., & Robinson, C. V. (2019). Membrane Protein–Lipid Interactions Probed Using Mass Spectrometry. *Annual Review of Biochemistry*, *88*(1), 85–111. https://doi.org/10.1146/annurev-biochem-013118-111508

Brough, Z., Zhao, Z., & Duong van Hoa, F. (2024). From bottom-up to cell surface proteomics: Detergents or no detergents, that is the question. *Biochemical Society Transactions*, *52*(3), 1253–1263. https://doi.org/10.1042/BST20231020

Brown, C., Ghosh, S., McAllister, R., Kumar, M., Walker, G., Sun, E., Aman, T., Panda, A., Kumar, S., Li, W., Coleman, J., Liu, Y., Rothman, J. E., Bhattacharyya, M., & Gupta, K. (2024). A proteome-wide quantitative platform for nanoscale spatially resolved extraction

of membrane proteins into native nanodiscs. *Nature Methods*, 1–10. https://doi.org/10.1038/s41592-024-02517-x

Carlson, M. L., Stacey, R. G., Young, J. W., Wason, I. S., Zhao, Z., Rattray, D. G., Scott, N., Kerr, C. H., Babu, M., Foster, L. J., & Duong Van Hoa, F. (2019). Profiling the Escherichia coli membrane protein interactome captured in Peptidisc libraries. *eLife*, *8*, e46615. https://doi.org/10.7554/eLife.46615

Carlson, M. L., Young, J. W., Zhao, Z., Fabre, L., Jun, D., Li, J., Li, J., Dhupar, H. S., Wason, I., Mills, A. T., Beatty, J. T., Klassen, J. S., Rouiller, I., & Duong, F. (2018). The Peptidisc, a simple method for stabilizing membrane proteins in detergent-free solution. *eLife*, *7*, e34085. https://doi.org/10.7554/eLife.34085

Caterina, M. J., Schumacher, M. A., Tominaga, M., Rosen, T. A., Levine, J. D., & Julius, D. (1997). The capsaicin receptor: A heat-activated ion channel in the pain pathway. *Nature*, *389*(6653), 816–824. https://doi.org/10.1038/39807

Cherepanov, D. A., Brady, N. G., Shelaev, I. V., Nguyen, J., Gostev, F. E., Mamedov, M. D., Nadtochenko, V. A., & Bruce, B. D. (2019). PSI-SMALP, a Detergent-free Cyanobacterial Photosystem I, Reveals Faster Femtosecond Photochemistry. *Biophysical Journal*, *118*(2), 337. https://doi.org/10.1016/j.bpj.2019.11.3391

Christoforou, A. L., & Lilley, K. S. (2012). Isobaric tagging approaches in quantitative proteomics: The ups and downs. *Analytical and Bioanalytical Chemistry*, *404*(4), 1029–1037. https://doi.org/10.1007/s00216-012-6012-9

Christoforou, A., & Lilley, K. S. (2011). Taming the isobaric tagging elephant in the room in quantitative proteomics. *Nature Methods*, *8*(11), 911–913. https://doi.org/10.1038/nmeth.1736

Ciută, A.-D., Nosol, K., Kowal, J., Mukherjee, S., Ramírez, A. S., Stieger, B., Kossiakoff, A. A., & Locher, K. P. (2023). Structure of human drug transporters OATP1B1 and OATP1B3. *Nature Communications*, *14*(1), 5774. https://doi.org/10.1038/s41467-023-41552-8

Colas, C., Ung, P. M.-U., & Schlessinger, A. (2016). SLC Transporters: Structure, Function, and Drug Discovery. *MedChemComm*, *7*(6), 1069–1081. https://doi.org/10.1039/C6MD00005C

Corey, R. A., Pyle, E., Allen, W. J., Watkins, D. W., Casiraghi, M., Miroux, B., Arechaga, I., Politis, A., & Collinson, I. (2018). Specific cardiolipin–SecY interactions are required for proton-motive force stimulation of protein secretion. *Proceedings of the National Academy of Sciences of the United States of America*, *115*(31), 7967–7972. https://doi.org/10.1073/pnas.1721536115

Cymer, F., Heijne, G. von, & White, S. H. (2014). Mechanisms of integral membrane protein insertion and folding. *Journal of Molecular Biology*, *427*(5), 999. https://doi.org/10.1016/j.jmb.2014.09.014

Danko, K., Lukasheva, E., Zhukov, V. A., Zgoda, V., & Frolov, A. (2022). Detergent-Assisted Protein Digestion—On the Way to Avoid the Key Bottleneck of Shotgun Bottom-Up Proteomics. *International Journal of Molecular Sciences*, *23*(22), 13903. https://doi.org/10.3390/ijms232213903

Dunham, W. H., Mullin, M., & Gingras, A.-C. (2012). Affinity-purification coupled to mass spectrometry: Basic principles and strategies. *PROTEOMICS*, *12*(10), 1576–1590. https://doi.org/10.1002/pmic.201100523

Eichacker, L. A., Granvogl, B., Mirus, O., Müller, B. C., Miess, C., & Schleiff, E. (2004). Hiding behind Hydrophobicity: TRANSMEMBRANE SEGMENTS IN MASS

SPECTROMETRY *. *Journal of Biological Chemistry*, *279*(49), 50915–50922. https://doi.org/10.1074/jbc.M405875200

Fagerberg, L., Jonasson, K., von Heijne, G., Uhlén, M., & Berglund, L. (2010). Prediction of the human membrane proteome. *PROTEOMICS*, *10*(6), 1141–1149. https://doi.org/10.1002/pmic.200900258

Fairman, J. W., Noinaj, N., & Buchanan, S. K. (2011). The structural biology of β-barrel membrane proteins: A summary of recent reports. *Current Opinion in Structural Biology*, *21*(4), 523. https://doi.org/10.1016/j.sbi.2011.05.005

Ferraro, G., Belvedere, R., Petrella, A., Tosco, A., Stork, B., Salamone, S., Minassi, A., Pollastro, F., Morretta, E., & Monti, M. C. (2022). Drug affinity-responsive target stability unveils filamins as biological targets for artemetin, an anti-cancer flavonoid. *Frontiers in Molecular Biosciences*, *9*. https://doi.org/10.3389/fmolb.2022.964295

Galazzo, L., Meier, G., Januliene, D., Parey, K., De Vecchis, D., Striednig, B., Hilbi, H., Schäfer, L. V., Kuprov, I., Moeller, A., Bordignon, E., & Seeger, M. A. (2022). The ABC transporter MsbA adopts the wide inward-open conformation in E. coli cells. *Science Advances*, *8*(41), eabn6845. https://doi.org/10.1126/sciadv.abn6845

Gao, K., Oerlemans, R., & Groves, M. R. (2020). Theory and applications of differential scanning fluorimetry in early-stage drug discovery. *Biophysical Reviews*, *12*(1), 85–104. https://doi.org/10.1007/s12551-020-00619-2

Ghisaidoobe, A. B. T., & Chung, S. J. (2014). Intrinsic Tryptophan Fluorescence in the Detection and Analysis of Proteins: A Focus on Förster Resonance Energy Transfer Techniques. *International Journal of Molecular Sciences*, *15*(12), Article 12. https://doi.org/10.3390/ijms151222518

Gooran, N., & Kopra, K. (2024). Fluorescence-Based Protein Stability Monitoring—A Review. *International Journal of Molecular Sciences*, *25*(3), 1764. https://doi.org/10.3390/ijms25031764

Guan, Z., Yates, N. A., & Bakhtiar, R. (2003). Detection and characterization of methionine oxidation in peptides by collision-induced dissociation and electron capture dissociation. *Journal of the American Society for Mass Spectrometry*, *14*(6), 605–613. https://doi.org/10.1016/S1044-0305(03)00201-0

Gupta, K., Li, J., Liko, I., Gault, J., Bechara, C., Wu, D., Hopper, J. T. S., Giles, K., Benesch, J. L. P., & Robinson, C. V. (2018). Identifying key membrane protein lipid interactions using mass spectrometry. *Nature Protocols*, *13*(5), Article 5. https://doi.org/10.1038/nprot.2018.014

Harraz, O. F., Klug, N. R., Senatore, A. J., Hill-Eubanks, D. C., & Nelson, M. T. (2022). Piezo1 Is a Mechanosensor Channel in Central Nervous System Capillaries. *Circulation Research*, *130*(10), 1531–1546. https://doi.org/10.1161/CIRCRESAHA.122.320827

Helbig, A. O., Heck, A. J. R., & Slijper, M. (2010). Exploring the membrane proteome—Challenges and analytical strategies. *Journal of Proteomics*, *73*(5), 868–878. https://doi.org/10.1016/j.jprot.2010.01.005

Heyden, M., Freites, J. A., Ulmschneider, M. B., White, S. H., & Tobias, D. J. (2012). Assembly and Stability of α-Helical Membrane Proteins. *Soft Matter*, *8*(30), 7742. https://doi.org/10.1039/C2SM25402F

Hill, R. Z., Loud, M. C., Dubin, A. E., Peet, B., & Patapoutian, A. (2022). PIEZO1 transduces mechanical itch in mice. *Nature*, *607*(7917), 104–110. https://doi.org/10.1038/s41586-022-04860-5

Hoare, M., Tan, R., Welle, K. A., Swovick, K., Hryhorenko, J. R., & Ghaemmaghami, S. (2024). Methionine Alkylation as an Approach to Quantify Methionine Oxidation Using Mass Spectrometry. *Journal of the American Society for Mass Spectrometry*, *35*(3), 433–440. https://doi.org/10.1021/jasms.3c00337

Huber, K. V. M., Olek, K. M., Müller, A. C., Tan, C. S. H., Bennett, K. L., Colinge, J., & Superti-Furga, G. (2015). Proteome-wide drug and metabolite interaction mapping by thermal-stability profiling. *Nature Methods*, *12*(11), Article 11. https://doi.org/10.1038/nmeth.3590

Jandu, R. S., Yu, H., Zhao, Z., Le, H. T., Kim, S., Huan, T., & Hoa, F. D. van. (2024). Capture of endogenous lipids in peptidiscs and effect on protein stability and activity. *iScience*, *27*(4). https://doi.org/10.1016/j.isci.2024.109382

Johnson, F. D., Hughes, C. S., Liu, A., Lockwood, W. W., & Morin, G. B. (2023). Tandem mass tag-based thermal proteome profiling for the discovery of drug-protein interactions in cancer cells. *STAR Protocols*, *4*(1), 102012. https://doi.org/10.1016/j.xpro.2022.102012

Kalxdorf, M., Günthner, I., Becher, I., Kurzawa, N., Knecht, S., Savitski, M. M., Eberl, H. C., & Bantscheff, M. (2021). Cell surface thermal proteome profiling tracks perturbations and drug targets on the plasma membrane. *Nature Methods*, *18*(1), Article 1. https://doi.org/10.1038/s41592-020-01022-1

Kawatkar, A., Schefter, M., Hermansson, N.-O., Snijder, A., Dekker, N., Brown, D. G., Lundbäck, T., Zhang, A. X., & Castaldi, M. P. (2019). CETSA beyond Soluble Targets: A Broad Application to Multipass Transmembrane Proteins. *ACS Chemical Biology*, *14*(9), 1913–1920. https://doi.org/10.1021/acschembio.9b00399

Kermani, A. A. (2021). A guide to membrane protein X-ray crystallography. *The FEBS Journal*, *288*(20), 5788–5804. https://doi.org/10.1111/febs.15676

Khunweeraphong, N., Stockner, T., & Kuchler, K. (2017). The structure of the human ABC transporter ABCG2 reveals a novel mechanism for drug extrusion. *Scientific Reports*, *7*(1), 13767. https://doi.org/10.1038/s41598-017-11794-w

Kotov, V., Bartels, K., Veith, K., Josts, I., Subhramanyam, U. K. T., Günther, C., Labahn, J., Marlovits, T. C., Moraes, I., Tidow, H., Löw, C., & Garcia-Alai, M. M. (2019). High-throughput stability screening for detergent-solubilized membrane proteins. *Scientific Reports*, *9*(1), Article 1. https://doi.org/10.1038/s41598-019-46686-8

Kubitz, R., Dröge, C., Stindt, J., Weissenberger, K., & Häussinger, D. (2012). The bile salt export pump (BSEP) in health and disease. *Clinics and Research in Hepatology and Gastroenterology*, *36*(6), 536–553. https://doi.org/10.1016/j.clinre.2012.06.006

Kuo, Y.-C., Chen, H., Shang, G., Uchikawa, E., Tian, H., Bai, X.-C., & Zhang, X. (2020). Cryo-EM structure of the PlexinC1/A39R complex reveals inter-domain interactions critical for ligand-induced activation. *Nature Communications*, *11*(1), Article 1. https://doi.org/10.1038/s41467-020-15862-0

Laganowsky, A., Reading, E., Allison, T. M., Ulmschneider, M. B., Degiacomi, M. T., Baldwin, A. J., & Robinson, C. V. (2014). Membrane proteins bind lipids selectively to modulate their structure and function. *Nature*, *510*(7503), Article 7503. https://doi.org/10.1038/nature13419

Lanzetta, P. A., Alvarez, L. J., Reinach, P. S., & Candia, O. A. (1979). An improved assay for nanomole amounts of inorganic phosphate. *Analytical Biochemistry*, *100*(1), 95–97. https://doi.org/10.1016/0003-2697(79)90115-5

Le Sueur, C., Hammarén, H. M., Sridharan, S., & Savitski, M. M. (2022). Thermal proteome profiling: Insights into protein modifications, associations, and functions. *Current Opinion in Chemical Biology, 71*, 102225. https://doi.org/10.1016/j.cbpa.2022.102225

Lee, J.-J., Park, Y. S., & Lee, K.-J. (2015). Hydrogen–deuterium exchange mass spectrometry for determining protein structural changes in drug discovery. *Archives of Pharmacal Research*, *38*(10), 1737–1745. https://doi.org/10.1007/s12272-015-0584-9

Lee, W.-H., Najjar, S. M., Kahn, C. R., & Hinds, T. D. (2023). Hepatic insulin receptor: New views on the mechanisms of liver disease. *Metabolism*, *145*, 155607. https://doi.org/10.1016/j.metabol.2023.155607

Lenoir, G., Dieudonné, T., Lamy, A., Lejeune, M., Vazquez-Ibar, J.-L., & Montigny, C. (2018). Screening of Detergents for Stabilization of Functional Membrane Proteins. *Current Protocols in Protein Science*, *93*(1), e59. https://doi.org/10.1002/cpps.59

Li, J., Van Vranken, J. G., Pontano Vaites, L., Schweppe, D. K., Huttlin, E. L., Etienne, C., Nandhikonda, P., Viner, R., Robitaille, A. M., Thompson, A. H., Kuhn, K., Pike, I., Bomgarden, R. D., Rogers, J. C., Gygi, S. P., & Paulo, J. A. (2020). TMTpro reagents: A set of isobaric labeling mass tags enables simultaneous proteome-wide measurements across 16 samples. *Nature Methods*, *17*(4), 399–404. https://doi.org/10.1038/s41592-020-0781-4

Liang, B., & Tamm, L. K. (2016). NMR as a tool to investigate the structure, dynamics and function of membrane proteins. *Nature Structural & Molecular Biology*, *23*(6), 468–474. https://doi.org/10.1038/nsmb.3226

Ligon, B. L. (2004). Penicillin: Its discovery and early development. *Seminars in Pediatric Infectious Diseases*, *15*(1), 52–57. https://doi.org/10.1053/j.spid.2004.02.001

Liu, H., Irobalieva, R. N., Kowal, J., Ni, D., Nosol, K., Bang-Sørensen, R., Lancien, L., Stahlberg, H., Stieger, B., & Locher, K. P. (2023). Structural basis of bile salt extrusion and small-molecule inhibition in human BSEP. *Nature Communications*, *14*(1), 7296. https://doi.org/10.1038/s41467-023-43109-1

Liu, M., & Dongre, A. (2021). Proper imputation of missing values in proteomics datasets for differential expression analysis. *Briefings in Bioinformatics*, *22*(3), bbaa112. https://doi.org/10.1093/bib/bbaa112

Liu, X., Salokas, K., Weldatsadik, R. G., Gawriyski, L., & Varjosalo, M. (2020). Combined proximity labeling and affinity purification−mass spectrometry workflow for mapping and visualizing protein interaction networks. *Nature Protocols*, *15*(10), 3182–3211. https://doi.org/10.1038/s41596-020-0365-x

Lu, Q., Zhang, Y., Hellner, J., Giannini, C., Xu, X., Pauwels, J., Ma, Q., Dejonghe, W., Han, H., Van de Cotte, B., Impens, F., Gevaert, K., De Smet, I., Friml, J., Molina, D. M., & Russinova, E. (2022). Proteome-wide cellular thermal shift assay reveals unexpected cross-talk between brassinosteroid and auxin signaling. *Proceedings of the National Academy of Sciences*, *119*(11), e2118220119. https://doi.org/10.1073/pnas.2118220119

Lyu, J., Liu, C., Zhang, T., Schrecke, S., Elam, N. P., Packianathan, C., Hochberg, G. K. A., Russell, D., Zhao, M., & Laganowsky, A. (2022). Structural basis for lipid and copper regulation of the ABC transporter MsbA. *Nature Communications*, *13*(1), 7291. https://doi.org/10.1038/s41467-022-34905-2

Malinovska, L., Cappelletti, V., Kohler, D., Piazza, I., Tsai, T.-H., Pepelnjak, M., Stalder, P., Dörig, C., Sesterhenn, F., Elsässer, F., Kralickova, L., Beaton, N., Reiter, L., de Souza, N., Vitek, O., & Picotti, P. (2023). Proteome-wide structural changes measured with

limited proteolysis-mass spectrometry: An advanced protocol for high-throughput applications. *Nature Protocols*, *18*(3), 659–682. https://doi.org/10.1038/s41596-022-00771-x

Martin, J., & Sawyer, A. (2019). Elucidating the Structure of Membrane Proteins. *BioTechniques*, *66*(4), 167–170. https://doi.org/10.2144/btn-2019-0030

Massart, J., Begriche, K., Hartman, J. H., & Fromenty, B. (2022). Role of Mitochondrial Cytochrome P450 2E1 in Healthy and Diseased Liver. *Cells*, *11*(2), 288. https://doi.org/10.3390/cells11020288

Mateus, A., Bobonis, J., Kurzawa, N., Stein, F., Helm, D., Hevler, J., Typas, A., & Savitski, M. M. (2018). Thermal proteome profiling in bacteria: Probing protein state in vivo. *Molecular Systems Biology*, *14*(7), e8242. https://doi.org/10.15252/msb.20188242

Mateus, A., Kurzawa, N., Becher, I., Sridharan, S., Helm, D., Stein, F., Typas, A., & Savitski, M. M. (2020). Thermal proteome profiling for interrogating protein interactions. *Molecular Systems Biology*, *16*(3), e9232. https://doi.org/10.15252/msb.20199232

Mateus, A., Määttä, T. A., & Savitski, M. M. (2017). Thermal proteome profiling: Unbiased assessment of protein state through heat-induced stability changes. *Proteome Science*, *15*(1), 13. https://doi.org/10.1186/s12953-017-0122-4

Maveyraud, L., & Mourey, L. (2020). Protein X-ray Crystallography and Drug Discovery. *Molecules*, *25*(5), Article 5. https://doi.org/10.3390/molecules25051030

Molina, D. M., Jafari, R., Ignatushchenko, M., Seki, T., Larsson, E. A., Dan, C., Sreekumar, L., Cao, Y., & Nordlund, P. (2013). Monitoring Drug Target Engagement in Cells and Tissues Using the Cellular Thermal Shift Assay. *Science*, *341*(6141), 84–87. https://doi.org/10.1126/science.1233606

Molina, D. M., & Nordlund, P. (2016). The Cellular Thermal Shift Assay: A Novel Biophysical Assay for In Situ Drug Target Engagement and Mechanistic Biomarker Studies. *Annual Review of Pharmacology and Toxicology*, *56*(Volume 56, 2016), 141–161. https://doi.org/10.1146/annurev-pharmtox-010715-103715

Motsa, B. B., & Stahelin, R. V. (2023). A beginner's guide to surface plasmon resonance. *The Biochemist*, *45*(1), 18–22. https://doi.org/10.1042/bio_2022_139

Muchiri, R. N., & van Breemen, R. B. (2021). Affinity selection–mass spectrometry for the discovery of pharmacologically active compounds from combinatorial libraries and natural products. *Journal of Mass Spectrometry*, *56*(5), e4647. https://doi.org/10.1002/jms.4647

Mueller, S., Kubicek, J., Merino, F., Hanisch, P., Maertens, B., & Lackmann, J.-W. (2023). *The bigger picture: Global analysis of solubilization performance of classical detergents versus new synthetic polymers utilizing shotgun proteomics* (p. 2023.07.11.548597). bioRxiv. https://doi.org/10.1101/2023.07.11.548597

Mullowney, M. W., Duncan, K. R., Elsayed, S. S., Garg, N., van der Hooft, J. J. J., Martin, N. I., Meijer, D., Terlouw, B. R., Biermann, F., Blin, K., Durairaj, J., Gorostiola González, M., Helfrich, E. J. N., Huber, F., Leopold-Messer, S., Rajan, K., de Rond, T., van Santen, J. A., Sorokina, M., … Medema, M. H. (2023). Artificial intelligence for natural product drug discovery. *Nature Reviews Drug Discovery*, *22*(11), 895–916. https://doi.org/10.1038/s41573-023-00774-7

Ou, X., Lao, Y., Xu, J., Wutthinitikornkit, Y., Shi, R., Chen, X., & Li, J. (2021). ATP Can Efficiently Stabilize Protein through a Unique Mechanism. *JACS Au*, *1*(10), 1766–1777. https://doi.org/10.1021/jacsau.1c00316

Pan, Y., Zhan, J., Jiang, Y., Xia, D., & Scheuring, S. (2023). A concerted ATPase cycle of the protein transporter AAA-ATPase Bcs1. *Nature Communications*, *14*(1), 6369. https://doi.org/10.1038/s41467-023-41806-5

Patching, S. G. (2014). Surface plasmon resonance spectroscopy for characterisation of membrane protein–ligand interactions and its potential for drug discovery. *Biochimica et Biophysica Acta (BBA) - Biomembranes*, *1838*(1, Part A), 43–55. https://doi.org/10.1016/j.bbamem.2013.04.028

Patel, A., Malinovska, L., Saha, S., Wang, J., Alberti, S., Krishnan, Y., & Hyman, A. A. (2017). ATP as a biological hydrotrope. *Science*, *356*(6339), 753–756. https://doi.org/10.1126/science.aaf6846

Pepelnjak, M., Velten, B., Näpflin, N., von Rosen, T., Palmiero, U. C., Ko, J. H., Maynard, H. D., Arosio, P., Weber-Ban, E., de Souza, N., Huber, W., & Picotti, P. (2024). In situ analysis of osmolyte mechanisms of proteome thermal stabilization. *Nature Chemical Biology*, *20*(8), 1053–1065. https://doi.org/10.1038/s41589-024-01568-7

Perrin, J., Werner, T., Kurzawa, N., Rutkowska, A., Childs, D. D., Kalxdorf, M., Poeckel, D., Stonehouse, E., Strohmer, K., Heller, B., Thomson, D. W., Krause, J., Becher, I., Eberl, H. C., Vappiani, J., Sevin, D. C., Rau, C. E., Franken, H., Huber, W., … Bergamini, G. (2020). Identifying drug targets in tissues and whole blood with thermal-shift profiling. *Nature Biotechnology*, *38*(3), 303–308. https://doi.org/10.1038/s41587-019-0388-4

Petersen, D. N., Hawkins, J., Ruangsiriluk, W., Stevens, K. A., Maguire, B. A., O'Connell, T. N., Rocke, B. N., Boehm, M., Ruggeri, R. B., Rolph, T., Hepworth, D., Loria, P. M., & Carpino, P. A. (2016). A Small-Molecule Anti-secretagogue of PCSK9 Targets the 80S

Ribosome to Inhibit PCSK9 Protein Translation. *Cell Chemical Biology*, *23*(11), 1362–1371. https://doi.org/10.1016/j.chembiol.2016.08.016

Piazza, I., Beaton, N., Bruderer, R., Knobloch, T., Barbisan, C., Chandat, L., Sudau, A., Siepe, I., Rinner, O., de Souza, N., Picotti, P., & Reiter, L. (2020). A machine learning-based chemoproteomic approach to identify drug targets and binding sites in complex proteomes. *Nature Communications*, *11*(1), 4200. https://doi.org/10.1038/s41467-020-18071-x

Piazza, I., Kochanowski, K., Cappelletti, V., Fuhrer, T., Noor, E., Sauer, U., & Picotti, P. (2018). A Map of Protein-Metabolite Interactions Reveals Principles of Chemical Communication. *Cell*, *172*(1), 358-372.e23. https://doi.org/10.1016/j.cell.2017.12.006

Pollock, N. L., Lloyd, J., Montinaro, C., Rai, M., & Dafforn, T. R. (2022). Conformational trapping of an ABC transporter in polymer lipid nanoparticles. *Biochemical Journal*, *479*(2), 145–159. https://doi.org/10.1042/BCJ20210312

Prudent, R., Annis, D. A., Dandliker, P. J., Ortholand, J.-Y., & Roche, D. (2020). Exploring new targets and chemical space with affinity selection-mass spectrometry. *Nature Reviews Chemistry*, *5*(1), 62–71. https://doi.org/10.1038/s41570-020-00229-2

Pytkowski, B., & Jagodzińska-Hamann, L. (1996). Effects of in vivo vanadate administration on calcium exchange and contractile force of rat ventricular myocardium. *Toxicology Letters*, *84*(3), 167–173. https://doi.org/10.1016/0378-4274(95)03625-3

Qin, S., Meng, M., Yang, D., Bai, W., Lu, Y., Peng, Y., Song, G., Wu, Y., Zhou, Q., Zhao, S., Huang, X., McCorvy, J. D., Cai, X., Dai, A., Roth, B. L., Hanson, M. A., Liu, Z.-J., Wang, M.-W., Stevens, R. C., & Shui, W. (2018). High-throughput identification of G

protein-coupled receptor modulators through affinity mass spectrometry screening. *Chemical Science*, *9*(12), 3192–3199. https://doi.org/10.1039/C7SC04698G

Rajarathnam, K., & Rösgen, J. (2013). Isothermal Titration Calorimetry of Membrane Proteins – Progress and Challenges. *Biochimica et Biophysica Acta*, *1838*(1), 10.1016/j.bbamem.2013.05.023. https://doi.org/10.1016/j.bbamem.2013.05.023

Ramos, A. D., Liang, Y. Y., Surova, O., Bacanu, S., Gerault, M.-A., Mandal, T., Ceder, S., Langebäck, A., Österroos, A., Ward, G. A., Bergh, J., Wiman, K. G., Lehmann, S., Prabhu, N., Lööf, S., & Nordlund, P. (2024). Proteome-wide CETSA reveals diverse apoptosis-inducing mechanisms converging on an initial apoptosis effector stage at the nuclear periphery. *Cell Reports*, *43*(10). https://doi.org/10.1016/j.celrep.2024.114784

Reinhard, F. B. M., Eberhard, D., Werner, T., Franken, H., Childs, D., Doce, C., Savitski, M. F., Huber, W., Bantscheff, M., Savitski, M. M., & Drewes, G. (2015). Thermal proteome profiling monitors ligand interactions with cellular membrane proteins. *Nature Methods*, *12*(12), Article 12. https://doi.org/10.1038/nmeth.3652

Renaud, J.-P., Chari, A., Ciferri, C., Liu, W., Rémigy, H.-W., Stark, H., & Wiesmann, C. (2018). Cryo-EM in drug discovery: Achievements, limitations and prospects. *Nature Reviews Drug Discovery*, *17*(7), 471–492. https://doi.org/10.1038/nrd.2018.77

Renaud, J.-P., Chung, C., Danielson, U. H., Egner, U., Hennig, M., Hubbard, R. E., & Nar, H. (2016). Biophysics in drug discovery: Impact, challenges and opportunities. *Nature Reviews Drug Discovery*, *15*(10), 679–698. https://doi.org/10.1038/nrd.2016.123

Rosenbaum, M. I., Clemmensen, L. S., Bredt, D. S., Bettler, B., & Strømgaard, K. (2020). Targeting receptor complexes: A new dimension in drug discovery. *Nature Reviews Drug Discovery*, *19*(12), 884–901. https://doi.org/10.1038/s41573-020-0086-4

Sarkar, C. A., Dodevski, I., Kenig, M., Dudli, S., Mohr, A., Hermans, E., & Plückthun, A. (2008). Directed evolution of a G protein-coupled receptor for expression, stability, and binding selectivity. *Proceedings of the National Academy of Sciences*, *105*(39), 14808–14813. https://doi.org/10.1073/pnas.0803103105

Saville, J. W., Troman, L., & Hoa, F. D. V. (2019). PeptiQuick, a One-Step Incorporation of Membrane Proteins into Biotinylated Peptidiscs for Streamlined Protein Binding Assays. *JoVE (Journal of Visualized Experiments)*, *153*, e60661. https://doi.org/10.3791/60661

Savitski, M. M., Mathieson, T., Zinn, N., Sweetman, G., Doce, C., Becher, I., Pachl, F., Kuster, B., & Bantscheff, M. (2013). Measuring and Managing Ratio Compression for Accurate iTRAQ/TMT Quantification. *Journal of Proteome Research*, *12*(8), 3586–3598. https://doi.org/10.1021/pr400098r

Savitski, M. M., Reinhard, F. B. M., Franken, H., Werner, T., Savitski, M. F., Eberhard, D., Molina, D. M., Jafari, R., Dovega, R. B., Klaeger, S., Kuster, B., Nordlund, P., Bantscheff, M., & Drewes, G. (2014). Tracking cancer drugs in living cells by thermal profiling of the proteome. *Science*, *346*(6205), 1255784. https://doi.org/10.1126/science.1255784

Schulze, R. J., Schott, M. B., Casey, C. A., Tuma, P. L., & McNiven, M. A. (2019). The cell biology of the hepatocyte: A membrane trafficking machine. *Journal of Cell Biology*, *218*(7), 2096–2112. https://doi.org/10.1083/jcb.201903090

Searle, B. C. (2024). Characterizing protein-protein interactions with thermal proteome profiling. *Current Opinion in Structural Biology*, *89*, 102946. https://doi.org/10.1016/j.sbi.2024.102946

Shao, S., & Hegde, R. S. (2011). Membrane Protein Insertion at the Endoplasmic Reticulum. *Annual Review of Cell and Developmental Biology*, *27*, 25. https://doi.org/10.1146/annurev-cellbio-092910-154125

Sharma, S., Zhou, R., Wan, L., Feng, S., Song, K., Xu, C., Li, Y., & Liao, M. (2021). Mechanism of LolCDE as a molecular extruder of bacterial triacylated lipoproteins. *Nature Communications*, *12*, 4687. https://doi.org/10.1038/s41467-021-24965-1

Shuken, S. R. (2023). An Introduction to Mass Spectrometry-Based Proteomics. *Journal of Proteome Research*, *22*(7), 2151–2171. https://doi.org/10.1021/acs.jproteome.2c00838

Siebenmorgen, T., Menezes, F., Benassou, S., Merdivan, E., Didi, K., Mourão, A. S. D., Kitel, R., Liò, P., Kesselheim, S., Piraud, M., Theis, F. J., Sattler, M., & Popowicz, G. M. (2024). MISATO: Machine learning dataset of protein–ligand complexes for structure-based drug discovery. *Nature Computational Science*, *4*(5), 367–378. https://doi.org/10.1038/s43588-024-00627-2

Spadaccini, R., Kaur, H., Becker-Baldus, J., & Glaubitz, C. (2018). The effect of drug binding on specific sites in transmembrane helices 4 and 6 of the ABC exporter MsbA studied by DNP-enhanced solid-state NMR. *Biochimica et Biophysica Acta (BBA) - Biomembranes*, *1860*(4), 833–840. https://doi.org/10.1016/j.bbamem.2017.10.017

Sridharan, S., Kurzawa, N., Werner, T., Günthner, I., Helm, D., Huber, W., Bantscheff, M., & Savitski, M. M. (2019). Proteome-wide solubility and thermal stability profiling reveals distinct regulatory roles for ATP. *Nature Communications*, *10*(1), Article 1. https://doi.org/10.1038/s41467-019-09107-y

Strickland, E. C., Geer, M. A., Tran, D. T., Adhikari, J., West, G. M., DeArmond, P. D., Xu, Y., & Fitzgerald, M. C. (2013). Thermodynamic analysis of protein-ligand binding

interactions in complex biological mixtures using the stability of proteins from rates of oxidation. *Nature Protocols*, *8*(1), 148–161. https://doi.org/10.1038/nprot.2012.146

Swinney, D. C. (2013). Phenotypic vs. Target-Based Drug Discovery for First-in-Class Medicines. *Clinical Pharmacology & Therapeutics*, *93*(4), 299–301. https://doi.org/10.1038/clpt.2012.236

Tang, W. K., Borgnia, M. J., Hsu, A. L., Esser, L., Fox, T., de Val, N., & Xia, D. (2020). Structures of AAA protein translocase Bcs1 suggest translocation mechanism of a folded protein. *Nature Structural & Molecular Biology*, *27*(2), 202–209. https://doi.org/10.1038/s41594-020-0373-0

Taylor, N. M. I., Manolaridis, I., Jackson, S. M., Kowal, J., Stahlberg, H., & Locher, K. P. (2017). Structure of the human multidrug transporter ABCG2. *Nature*, *546*(7659), 504–509. https://doi.org/10.1038/nature22345

The mouse genome. (2002). *Nature*, *420*(6915), 510–510. https://doi.org/10.1038/420510a

Thompson, A., Schäfer, J., Kuhn, K., Kienle, S., Schwarz, J., Schmidt, G., Neumann, T., & Hamon, C. (2003). Tandem Mass Tags: A Novel Quantification Strategy for Comparative Analysis of Complex Protein Mixtures by MS/MS. *Analytical Chemistry*, *75*(8), 1895–1904. https://doi.org/10.1021/ac0262560

Ting, L., Rad, R., Gygi, S. P., & Haas, W. (2011). MS3 eliminates ratio distortion in isobaric multiplexed quantitative proteomics. *Nature Methods*, *8*(11), 937–940. https://doi.org/10.1038/nmeth.1714

Toporowska, J., Kapoor, P., Musgaard, M., Gherbi, K., Sengmany, K., Qu, F., Soave, M., Yen, H.-Y., Hansen, K., Jazayeri, A., Hopper, J. T. S., & Politis, A. (2024). Ligand-induced conformational changes in the β1-adrenergic receptor revealed by hydrogen-deuterium

exchange mass spectrometry. *Nature Communications*, *15*(1), 8993. https://doi.org/10.1038/s41467-024-53161-0

Vecchio, I., Tornali, C., Bragazzi, N. L., & Martini, M. (2018). The Discovery of Insulin: An Important Milestone in the History of Medicine. *Frontiers in Endocrinology*, *9*, 613. https://doi.org/10.3389/fendo.2018.00613

Vu, H. N., Situ, A. J., & Ulmer, T. S. (2021). Isothermal Titration Calorimetry of Membrane Proteins. In I. Schmidt-Krey & J. C. Gumbart (Eds.), *Structure and Function of Membrane Proteins* (pp. 69–79). Springer US. https://doi.org/10.1007/978-1-0716-1394-8_5

Wagner, S., Baars, L., Ytterberg, A. J., Klussmeier, A., Wagner, C. S., Nord, O., Nygren, P.-Å., van Wijk, K. J., & de Gier, J.-W. (2007). Consequences of Membrane Protein Overexpression in *Escherichia coli**. *Molecular & Cellular Proteomics*, *6*(9), 1527–1550. https://doi.org/10.1074/mcp.M600431-MCP200

Wagner, S., Bader, M. L., Drew, D., & de Gier, J.-W. (2006). Rationalizing membrane protein overexpression. *Trends in Biotechnology*, *24*(8), 364–371. https://doi.org/10.1016/j.tibtech.2006.06.008

Ward, A., Reyes, C. L., Yu, J., Roth, C. B., & Chang, G. (2007). Flexibility in the ABC transporter MsbA: Alternating access with a twist. *Proceedings of the National Academy of Sciences*, *104*(48), 19005–19010. https://doi.org/10.1073/pnas.0709388104

Werner, T., Becher, I., Sweetman, G., Doce, C., Savitski, M. M., & Bantscheff, M. (2012). High-resolution enabled TMT 8-plexing. *Analytical Chemistry*, *84*(16), 7188–7194. https://doi.org/10.1021/ac301553x

Wiśniewski, J. R., Vildhede, A., Norén, A., & Artursson, P. (2016). In-depth quantitative analysis and comparison of the human hepatocyte and hepatoma cell line HepG2 proteomes. *Journal of Proteomics*, *136*, 234–247. https://doi.org/10.1016/j.jprot.2016.01.016

Yang, D., Zhou, Q., Labroska, V., Qin, S., Darbalaei, S., Wu, Y., Yuliantie, E., Xie, L., Tao, H., Cheng, J., Liu, Q., Zhao, S., Shui, W., Jiang, Y., & Wang, M.-W. (2021). G protein-coupled receptors: Structure- and function-based drug discovery. *Signal Transduction and Targeted Therapy*, *6*(1), 1–27. https://doi.org/10.1038/s41392-020-00435-w

Yang, X.-X., Xu, F., Wang, D., Yang, Z.-W., Tan, H.-R., Shang, M.-Y., Wang, X., & Cai, S.-Q. (2015). Development of a mitochondria-based centrifugal ultrafiltration/liquid chromatography/mass spectrometry method for screening mitochondria-targeted bioactive constituents from complex matrixes: Herbal medicines as a case study. *Journal of Chromatography A*, *1413*, 33–46. https://doi.org/10.1016/j.chroma.2015.08.014

Yang, Z., Han, S., Keller, M., Kaiser, A., Bender, B. J., Bosse, M., Burkert, K., Kögler, L. M., Wifling, D., Bernhardt, G., Plank, N., Littmann, T., Schmidt, P., Yi, C., Li, B., Ye, S., Zhang, R., Xu, B., Larhammar, D., … Wu, B. (2018). Structural basis of ligand binding modes at the neuropeptide Y Y1 receptor. *Nature*, *556*(7702), 520–524. https://doi.org/10.1038/s41586-018-0046-x

Yang, Z., Wang, C., Zhou, Q., An, J., Hildebrandt, E., Aleksandrov, L. A., Kappes, J. C., DeLucas, L. J., Riordan, J. R., Urbatsch, I. L., Hunt, J. F., & Brouillette, C. G. (2014). Membrane protein stability can be compromised by detergent interactions with the extramembranous soluble domains. *Protein Science : A Publication of the Protein Society*, *23*(6), 769–789. https://doi.org/10.1002/pro.2460

Ye, Y., Li, K., Ma, Y., Zhang, X., Li, Y., Yu, T., Wang, Y., & Ye, M. (2023). The Introduction of Detergents in Thermal Proteome Profiling Requires Lowering the Applied Temperatures for Efficient Target Protein Identification. *Molecules*, *28*(12), Article 12. https://doi.org/10.3390/molecules28124859

Yen, H.-Y., Hoi, K. K., Liko, I., Hedger, G., Horrell, M. R., Song, W., Wu, D., Heine, P., Warne, T., Lee, Y., Carpenter, B., Plückthun, A., Tate, C. G., Sansom, M. S. P., & Robinson, C. V. (2018). PIP2 stabilises active states of GPCRs and enhances the selectivity of G-protein coupling. *Nature*, *559*(7714), 423–427. https://doi.org/10.1038/s41586-018-0325-6

Yen, H.-Y., Hopper, J. T. S., Liko, I., Allison, T. M., Zhu, Y., Wang, D., Stegmann, M., Mohammed, S., Wu, B., & Robinson, C. V. (2017). Ligand binding to a G protein–coupled receptor captured in a mass spectrometer. *Science Advances*. https://doi.org/10.1126/sciadv.1701016

Young, J. W. (2023). Recent advances in membrane mimetics for membrane protein research. *Biochemical Society Transactions*, *51*(3), 1405–1416. https://doi.org/10.1042/BST20230164

Young, J. W., Pfitzner, E., van Wee, R., Kirschbaum, C., Kukura, P., & Robinson, C. V. (2024). Characterization of membrane protein interactions by peptidisc-mediated mass photometry. *iScience*, *27*(2), 108785. https://doi.org/10.1016/j.isci.2024.108785

Young, J. W., Wason, I. S., Zhao, Z., Kim, S., Aoki, H., Phanse, S., Rattray, D. G., Foster, L. J., Babu, M., & Duong van Hoa, F. (2022). Development of a Method Combining Peptidiscs and Proteomics to Identify, Stabilize, and Purify a Detergent-Sensitive Membrane Protein

Assembly. *Journal of Proteome Research*, *21*(7), 1748–1758. https://doi.org/10.1021/acs.jproteome.2c00129

Young, J. W., Wason, I. S., Zhao, Z., Rattray, D. G., Foster, L. J., & Duong Van Hoa, F. (2020). His-Tagged Peptidiscs Enable Affinity Purification of the Membrane Proteome for Downstream Mass Spectrometry Analysis. *Journal of Proteome Research*, *19*(7), 2553–2562. https://doi.org/10.1021/acs.jproteome.0c00022

Young, J. W., Zhao, Z., Wason, I. S., & Duong van Hoa, F. (2023). A Dual Detergent Strategy to Capture a Bacterial Outer Membrane Proteome in Peptidiscs for Characterization by Mass Spectrometry and Binding Assays. *Journal of Proteome Research*, *22*(5), 1537–1545. https://doi.org/10.1021/acs.jproteome.2c00560

Zhan, J., Zeher, A., Huang, R., Tang, W. K., Jenkins, L. M., & Xia, D. (2024). Conformations of Bcs1L undergoing ATP hydrolysis suggest a concerted translocation mechanism for folded iron-sulfur protein substrate. *Nature Communications*, *15*(1), 4655. https://doi.org/10.1038/s41467-024-49029-y

Zhang, B., Käll, L., & Zubarev, R. A. (2016). DeMix-Q: Quantification-Centered Data Processing Workflow*. *Molecular & Cellular Proteomics*, *15*(4), 1467–1478. https://doi.org/10.1074/mcp.O115.055475

Zhang, N., & Li, L. (2004). Effects of common surfactants on protein digestion and matrix-assisted laser desorption/ionization mass spectrometric analysis of the digested peptides using two-layer sample preparation. *Rapid Communications in Mass Spectrometry*, *18*(8), 889–896. https://doi.org/10.1002/rcm.1423

Zhang, X. C., & Han, L. (2016). How does a β-barrel integral membrane protein insert into the membrane? *Protein & Cell*, *7*(7), 471. https://doi.org/10.1007/s13238-016-0273-6

Zhao, L.-H., Ma, S., Sutkeviciute, I., Shen, D.-D., Zhou, X. E., de Waal, P. W., Li, C.-Y., Kang, Y., Clark, L. J., Jean-Alphonse, F. G., White, A. D., Yang, D., Dai, A., Cai, X., Chen, J., Li, C., Jiang, Y., Watanabe, T., Gardella, T. J., … Zhang, Y. (2019). Structure and dynamics of the active human parathyroid hormone receptor-1. *Science (New York, N.Y.)*, *364*(6436), 148–153. https://doi.org/10.1126/science.aav7942

Zhao, Z., Khurana, A., Antony, F., Young, J. W., Hewton, K. G., Brough, Z., Zhong, T., Parker, S. J., & Duong van Hoa, F. (2023). A Peptidisc-Based Survey of the Plasma Membrane Proteome of a Mammalian Cell. *Molecular & Cellular Proteomics : MCP*, *22*(8), 100588. https://doi.org/10.1016/j.mcpro.2023.100588

Zhou, A., Rohou, A., Schep, D. G., Bason, J. V., Montgomery, M. G., Walker, J. E., Grigorieff, N., & Rubinstein, J. L. (2015). Structure and conformational states of the bovine mitochondrial ATP synthase by cryo-EM. *eLife*, *4*, e10180. https://doi.org/10.7554/eLife.10180

Zorman, S., Botte, M., Jiang, Q., Collinson, I., & Schaffitzel, C. (2015). Advances and challenges of membrane–protein complex production. *Current Opinion in Structural Biology*, *32*, 123–130. https://doi.org/10.1016/j.sbi.2015.03.010

Appendices

Appendix A

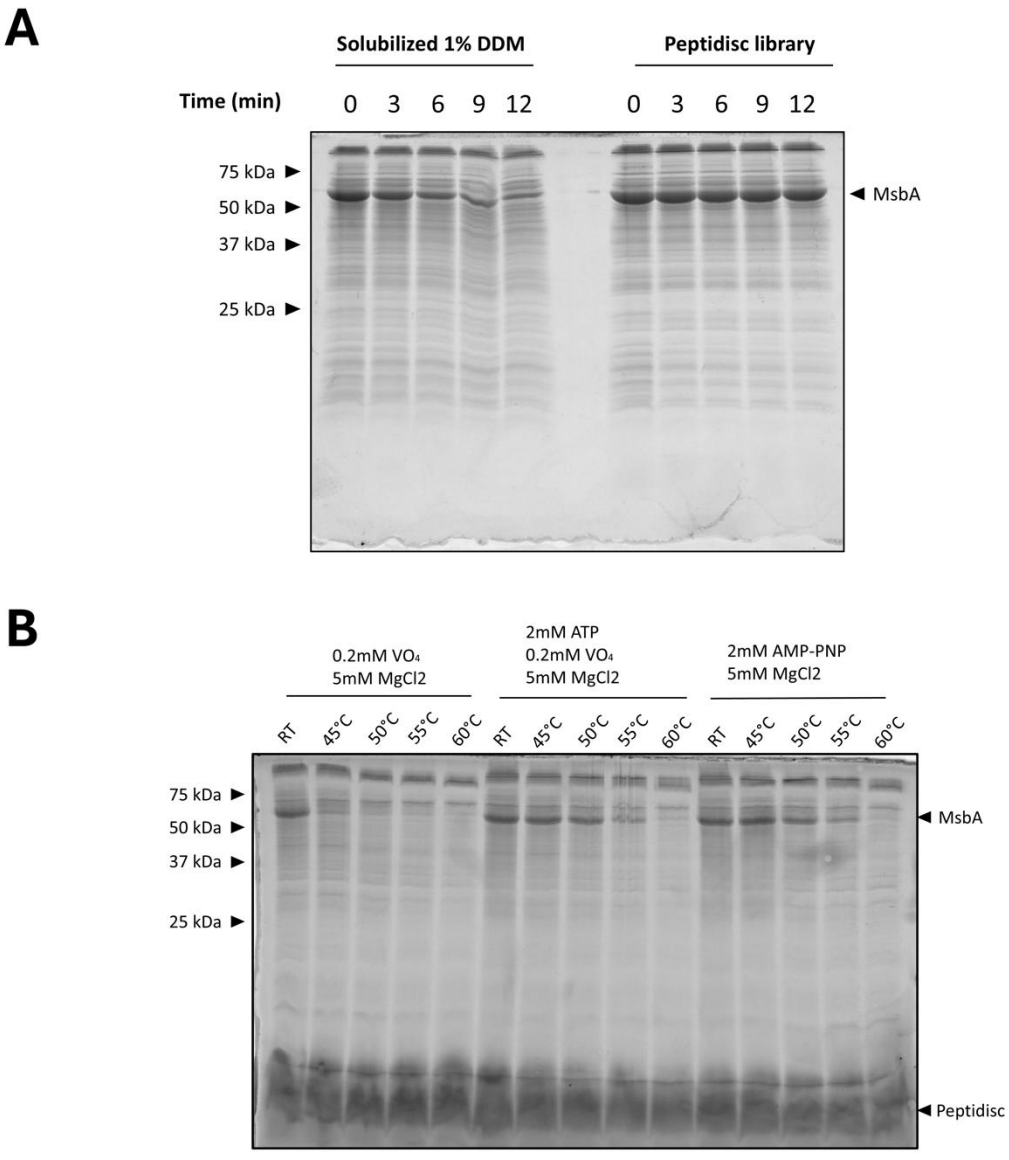

Supplementary Figure 1: Thermal stability of MsbA in detergent or with ligands. (**A**) The *E. coli* membrane fraction enriched for MsbA was solubilized with 1% DDM or reconstituted in Peptidisc. The detergent extract and Peptidisc library were incubated at 45°C for the indicated

times. After centrifugation, the supernatants were analyzed on 15% SDS-PAGE and visualized with Coomassie blue staining. (**B**) The Peptidisc library prepared in (A) was incubated with ATP-VO_4 or AMP-PNP at the indicated temperature. Supernatants were analyzed on 15% SDS-PAGE and visualized with Coomassie blue staining.

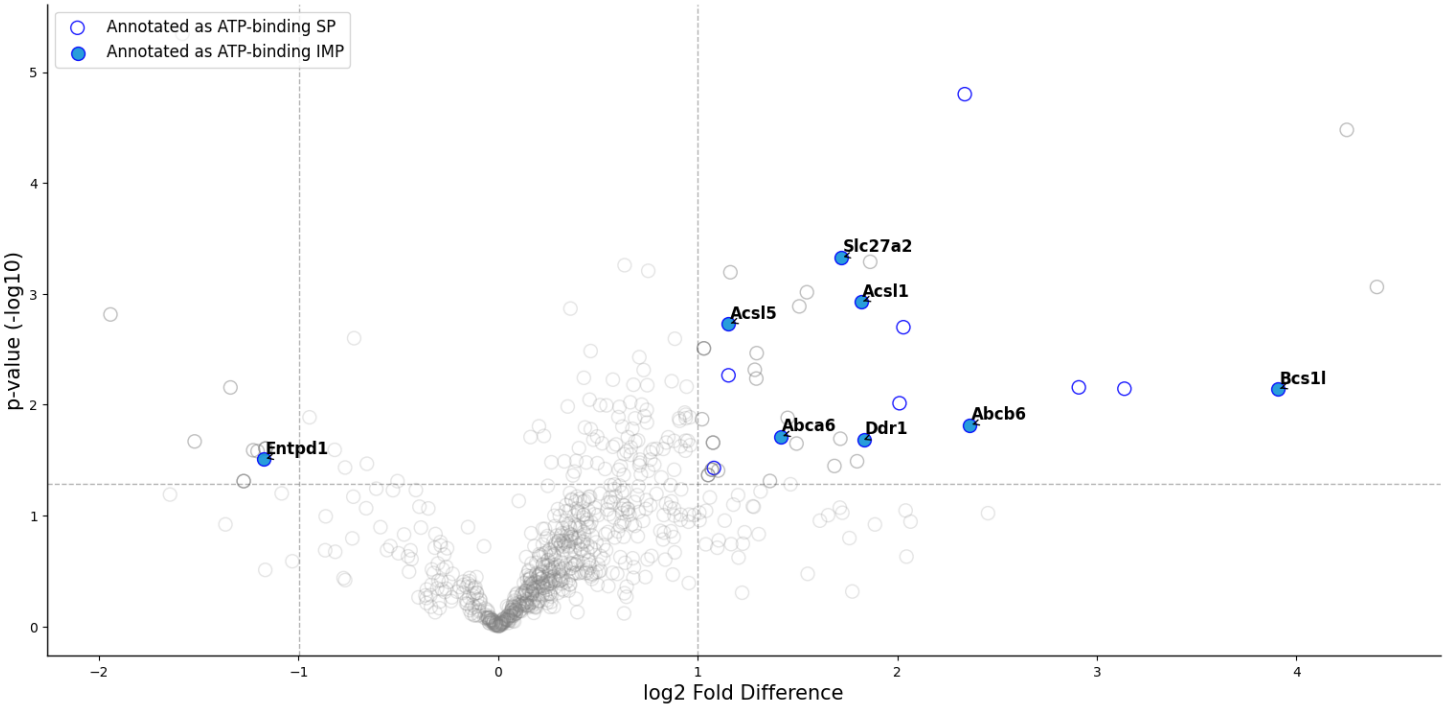

Supplementary Figure 2: Volcano plot of stabilized and destabilized proteins at 51°C in the presence of AMP-PNP. Soluble proteins (SP) annotated as ATP-binding proteins are presented as hollow blue circles, and IMPs annotated as ATP-binding are presented as solid blue circles. The mean value is obtained from three replicates at the temperature exposure assay (n = 3).

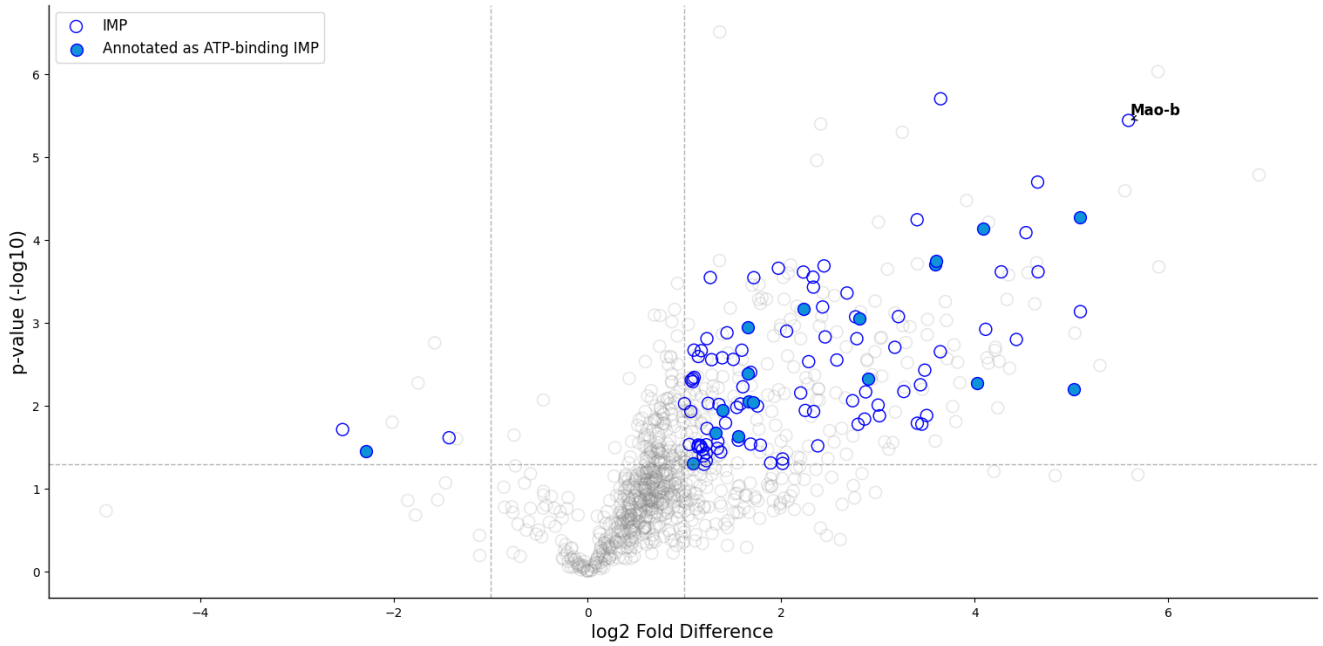

Supplementary Figure 3: Volcano plot of stabilized and destabilized proteins at 64°C in the presence of ATP-VO_4. Stabilized and destabilized IMPs are represented by hollow blue circles and IMPs annotated as ATP-binding are represented by solid blue circles with label on Mao-B. The mean value is obtained from three replicates at the temperature exposure assay (n = 3).

Supplementary Table 1: Protein abundances in peptidisc library. Number of proteins identified in the mouse liver peptidisc library at the indicated temperature to assess loss of IMPs compared to global protein abundance. At least two unique peptides were identified for each protein (n = 2).

Temperature	Total protein	Total IMP
Room temperature	998 ± 2	470 ± 3 (47%)
45°C	892 ± 11	425 ± 1 (48%)
50°C	810 ± 16	385 ± 7 (48%)
55°C	734 ± 46	354 ± 22 (48%)
60°C	566 ± 33	276 ± 11 (49%)
65°C	524 ± 4	264 ± 3 (50%)